Phosphorylation of Myosin-binding Subunit (MBS) of Myosin Phosphatase by Rho-Kinase In Vivo

Yoji Kawano,* Yuko Fukata,* Noriko Oshiro,* Mutsuki Amano,* Toshikazu Nakamura,‡ Masaaki Ito,§ Fumio Matsumura,‖ Masaki Inagaki,¶ and Kozo Kaibuchi*

*Division of Signal Transduction, Nara Institute of Science and Technology, 8916-5 Takayama, Ikoma 630-0101, Japan; ‡Division of Biochemistry, Osaka University Medical School, Suita, Osaka 565-0871, Japan; §The First Department of Internal Medicine, Mie University School of Medicine, Edobashi, Tsu, Mie 514-8507, Japan; ‖Department of Molecular Biology and Biochemistry, Rutgers University, Piscataway, New Jersey 08855; and ¶Laboratory of Biochemistry, Aichi Cancer Center Research Institute, Chikusa-ku, Nagoya 464-0021, Japan

Abstract. Rho-associated kinase (Rho-kinase), which is activated by the small GTPase Rho, phosphorylates myosin-binding subunit (MBS) of myosin phosphatase and thereby inactivates the phosphatase activity in vitro. Rho-kinase is thought to regulate the phosphorylation state of the substrates including myosin light chain (MLC), ERM (ezrin/radixin/moesin) family proteins and adducin by their direct phosphorylation and by the inactivation of myosin phosphatase. Here we identified the sites of phosphorylation of MBS by Rho-kinase as Thr-697, Ser-854 and several residues, and prepared antibody that specifically recognized MBS phosphorylated at Ser-854. We found by use of this antibody that the stimulation of MDCK epithelial cells with tetradecanoylphorbol-13-acetate (TPA) or hepatocyte growth factor (HGF) induced the phosphorylation of MBS at Ser-854 under the conditions in which membrane ruffling and cell migration were induced. Pretreatment of the cells with *Botulinum* C3 ADP-ribosyltransferase (C3), which is thought to interfere with Rho functions, or Rho-kinase inhibitors inhibited the TPA- or HGF-induced MBS phosphorylation. The TPA stimulation enhanced the immunoreactivity of phosphorylated MBS in the cytoplasm and membrane ruffling area of MDCK cells. In migrating MDCK cells, phosphorylated MBS as well as phosphorylated MLC at Ser-19 were localized in the leading edge and posterior region. Phosphorylated MBS was localized on actin stress fibers in REF52 fibroblasts. The microinjection of C3 or dominant negative Rho-kinase disrupted stress fibers and weakened the accumulation of phosphorylated MBS in REF52 cells. During cytokinesis, phosphorylated MBS, MLC and ERM family proteins accumulated at the cleavage furrow, and the phosphorylation level of MBS at Ser-854 was increased. Taken together, these results indicate that MBS is phosphorylated by Rho-kinase downstream of Rho in vivo, and suggest that myosin phosphatase and Rho-kinase spatiotemporally regulate the phosphorylation state of Rho-kinase substrates including MLC and ERM family proteins in vivo in a cooperative manner.

Key words: myosin-binding subunit of myosin phosphatase • Rho-associated kinase • Rho • phosphorylation • cytokinesis

EVIDENCE is accumulating that the small GTPase Rho plays crucial roles in the regulation of various cellular functions including stress fiber and focal adhesion formation (Ridley and Hall, 1992, 1994), smooth muscle contraction (Hirata et al., 1992; Gong et al., 1996), neurite retraction (Nishiki et al., 1990; Jalink et al., 1994), microvilli formation (Shaw et al., 1998), cytokinesis (Kishi et al., 1993; Mabuchi et al., 1993), cell migration (Takaishi et al., 1993, 1994), and gene expression (Hill et al., 1995). Rho cycles between GDP-bound inactive and GTP-bound active forms, and the GTP-bound form binds to specific targets and then exerts its biological functions (Van Aelst and D'Souza-Schorey, 1997; Hall, 1998; Kaibuchi et al., 1999). Numerous putative Rho targets have been identified, including protein kinase N (Amano et al., 1996b; Watanabe et al., 1996), Rho-kinase/ROKα/ROCK II (Leung et al., 1995; Ishizaki et al., 1996; Matsui et al., 1996), myo-

sin-binding subunit (MBS)[1] of myosin phosphatase (Kimura et al., 1996), p140mDia (Watanabe et al., 1997), citron (Madaule et al., 1995), citron kinase (Madaule et al., 1998), rhophilin (Watanabe et al., 1996), rhotekin (Reid et al., 1996), Kv1.2 (Cachero et al., 1998), and phospholipase D (Singer et al., 1997). ROKβ/ROCK I is an isoform of Rho-kinase (Ishizaki et al., 1996; Leung et al., 1996). Myosin phosphatase is composed of MBS, a 37-kD type 1 phosphatase catalytic subunit and a 20-kD regulatory subunit (Alessi et al., 1992; Hartshorne et al., 1998). Myosin phosphatase binds to phosphorylated myosin light chain (MLC) via MBS and dephosphorylates MLC. Rho-kinase phosphorylates MBS, which leads to the inactivation of myosin phosphatase in vitro (Kimura et al., 1996). Rho-kinase by itself phosphorylates MLC at the same site that is phosphorylated by MLC-kinase, and activates myosin ATPase (Amano et al., 1996a). Thus, Rho-kinase and myosin phosphatase appear to regulate the phosphorylation level of MLC, cooperatively. Consistently, the addition of the dominant active Rho-kinase to permeabilized vascular smooth muscle induces a contraction through MLC phosphorylation (Kureishi et al., 1997). In non-muscle cells, the expression of dominant active Rho-kinase increases the MLC phosphorylation, which in turn induces stress fiber and focal adhesion formation in fibroblasts (Leung et al., 1996; Amano et al., 1997; Chihara et al., 1997; Ishizaki et al., 1997), and neurite retraction in neuronal cells (Amano et al., 1998; Hirose et al., 1998; Katoh et al., 1998). In addition to MLC and MBS, Rho-kinase phosphorylates ERM (ezrin/radixin/moesin) family proteins and adducin in vitro (Matsui et al., 1998; Kimura et al., 1998). Myosin phosphatase interacts with both ERM family proteins and adducin through MBS, and dephosphorylates the phosphorylated ERM family proteins and adducin (Fukata et al., 1998; Kimura et al., 1998). The phosphatase activity toward ERM family proteins and adducin is inhibited when MBS is phosphorylated by Rho-kinase as described for MLC (Fukata et al., 1998; Kimura et al., 1998). Moreover, we have found that the phosphorylation of moesin and adducin by Rho-kinase plays critical roles in the formation of microvilli-like structures in fibroblasts (Oshiro et al., 1998) and in membrane ruffling in MDCK cells (Fukata et al., 1999), respectively. Based on these observations, we have proposed the dual regulation model in which myosin phosphatase and Rho-kinase cooperatively regulate the phosphorylation state of the substrates including MLC, adducin and moesin downstream of Rho. However, it remains to be clarified how MBS phosphorylation is regulated downstream of Rho in intact cells.

In this study, we determined the sites of phosphorylation of MBS by Rho-kinase, and prepared antibody that specifically recognized MBS phosphorylated at Ser-854, which was the specific site for Rho-kinase, to understand

how MBS phosphorylation is regulated in vivo. We found by use of this antibody that MBS was phosphorylated by Rho-kinase downstream of Rho in vivo, and that phosphorylated MBS was localized in the nucleus, cytoplasm and membrane ruffling area in TPA-stimulated MDCK cells, on stress fibers in interphase REF52 cells, and at the cleavage furrow in mitotic MDCK cells.

Materials and Methods

Materials and Chemicals

The expression plasmid of *Botulinum* C3 ADP-ribosyltransferase (pGEX-C3) was kindly provided by Dr. A. Hall (University College London, London, UK). The MDCK cells and the cDNA-encoding mouse moesin (1–577 amino acids [aa]) were gifts from Dr. S. Tsukita (Kyoto University, Kyoto, Japan). Monoclonal mouse anti-MBS Ab (anti-mMBS Ab; antigen: 371–511 aa of M130) was kindly provided by Dr. D.J. Hartshorne (University of Arizona, Tuscon, Arizona; Trinkle-Mulcahy et al., 1995; Murata et al., 1997). HA1077 was kindly provided by Asahi Chemical Industry (Shizuoka, Japan). Y-32885 was synthesized as described (Uehata et al., 1997). Human recombinant hepatocyte growth factor (HGF) was produced and purified as described (Nakamura et al., 1989; Seki et al., 1990). TM71 (Goto et al., 1998), anti-pp2b Ab (Matsumura et al., 1998), anti-pT558 Ab (Oshiro et al., 1998), anti-pT445 Ab (Fukata et al., 1999), and polyclonal rabbit anti-MBS antibodies (anti-pnMBS Ab; antigen: 1–647 aa of M130 [Shimizu et al., 1994]/anti-pcMBS Ab; antigen: 758–1032 aa of Rat3 MBS) were generated. A rabbit polyclonal antibody against ERM (ezrin/radixin/moesin) family proteins (anti-ERM Ab) was generated as follows. Glutathione-*S*-transferase-mouse moesin (GST-mouse moesin; 357–577 aa) was produced and purified from *Escherichia coli* as an antigen. The obtained antiserum was then affinity-purified against mouse moesin (357–577 aa). Anti-ERM Ab specifically recognized ERM family proteins (data not shown). Protein kinase C (PKC) was prepared from rat brain as described (Kitano et al., 1986). Phosphatidyl serine, bisbenzimide Hoechst, anti-MLC Ab, nocodazole, and $N^6,2'$-*O*-dibutyryladenosine $3':5'$-cyclic monophosphate (dibutyryl cAMP) were purchased from Sigma Chemical Co. γ-[^{32}P]ATP was purchased from Amersham Corp.

Tetradecanoylphorbol-13-acetate (TPA) and calyculin A were purchased from Wako Pure Chemical Industries, Ltd. All materials used in the nucleic acid study were purchased from Takara Shuzo Co. Other materials and chemicals were obtained from commercial sources.

Preparation of Recombinant Proteins

GST-catalytic domain of Rho-kinase (GST-CAT; 6–553 aa) and full-length Rat3 MBS (1–1032 aa; Johnson et al., 1997) were produced in *Spodoptera frugiperda* cells in a baculovirus system and purified as described (Matsuura et al., 1987; Amano et al., 1996a; Fukata et al., 1998). Maltose-binding protein-RB/PH(TT) [MBP-RB/PH(TT); 941–1388 aa], GST-MBS-NH$_2$-terminal domain (GST-MBS-NT; 1–763 aa), GST-MBS-COOH-terminal domain (GST-MBS-CT; 758–1032 aa), GST-MBS-CT$^{S854A, T855A}$ (GST-MBS-CT AA), GST-RhoA^{141} and GST-C3 were produced and purified from *E. coli.* For microinjection, GST-C3 and GST-RhoA^{141} were cleaved with thrombin, and purified to remove the GST. MBP-RB/PH(TT), C3 and RhoA^{141} were concentrated, and during the concentration the buffer was replaced by microinjection buffer (20 mM Tris-HCl at pH 7.4, 20 mM NaCl, 1 mM MgCl$_2$, 0.1 mM EDTA, and 5 mM 2-mercaptoethanol). For incubation, the buffer of C3 was replaced by PBS. The guanosine $5'$-(3-*O*-thio)triphosphate (GTPγS) bound form of RhoA^{141} was prepared as described (Takaishi et al., 1993).

Phosphorylation Assay and Determination of the Sites of Phosphorylation of MBS by Rho-Kinase

The kinase reaction for Rho-kinase was carried out in 50 μl of kinase buffer A (50 mM Tris-HCl at pH 7.5, 5 mM MgCl$_2$, 1 mM EDTA, 1 mM EGTA, and 1 mM DTT) containing 100 μM γ-[^{32}P]ATP (1–20 GBq/mmol), 5 pmol of GST-CAT and 20 pmol of GST-MBS-NT, GST-MBS-CT, GST-MBS-CT AA, or full-length MBS. The kinase reaction for PKC was carried out in 50 μl of kinase buffer B (25 mM Tris-HCl at pH 7.5, 4 mM MgCl$_2$, 400 nM CaCl$_2$, 150 nM TPA, 10 μg/ml phosphatidyl serine,

and 1 mM DTT) containing 100 μM γ-[^{32}P]ATP (1–20 GBq/mmol), 5 pmol of PKC, and 20 pmol of full-length MBS. After an incubation for 15 min at 30°C, the reaction products were boiled in SDS sample buffer and aliquots of the reaction products were subjected to SDS-PAGE. The radiolabeled bands were visualized and estimated by an image analyzer (BAS-2000; Fuji).

To determine the sites of phosphorylation of MBS, the recombinant full-length MBS (1 nmol of protein) was phosphorylated with GST-CAT (200 pmol of protein) in 1 ml of kinase buffer A containing 100 μM γ-[^{32}P]ATP for 1 h at 30°C, and the reaction product was digested with *Achromobacter* protease I at 37°C for 20 h. The obtained peptides were applied onto a C18 reverse phase column (SG120; 4.6 × 250 mm; Shiseido) and eluted with a linear gradient of 0–48% acetonitrile for 100 min at a flow rate of 1.0 ml/min by high-performance liquid chromatography (System Gold; Beckman). The radioactive peptides were separated and phosphoamino acid sequencing was carried out with a peptide sequencer (PPSQ-10; Shimazu). The fractions obtained from each Edoman degradation cycle were measured for ^{32}P in a Beckman liquid scintillation counter.

Production of Site- and Phosphorylation State-specific Antibody for MBS

A rabbit polyclonal antibody against MBS phosphorylated at Ser-854 (anti-pS854 Ab) was prepared as described (Inagaki, M., et al., 1997). The phosphopeptide Cys-Arg[849]-Glu-Lys-Arg-Arg-phosphoSer[854]-Thr-Gly-Val-Ser-Phe[859] was chemically synthesized as an antigen and bound to the carrier protein, keyhole limpet hemocyanin at the NH$_2$-terminal cysteine residue, by Peptide Institute Inc. The obtained antiserum was then affinity-purified against the phosphopeptide.

Cell Culture

MDCK cells were grown in DME containing 10% calf serum, penicillin and streptomycin in an air-5% CO$_2$ atmosphere at constant humidity. REF52 cells were grown in DME containing 10% fetal bovine serum, penicillin, and streptomycin in an air-5% CO$_2$ atmosphere at constant humidity.

Detection of Phosphorylated MBS in MDCK Cells by Immunoblot Analysis

We employed the conditions for C3 treatment as described (Nishiki et al., 1990; Morii and Narumiya, 1995; Amano et al., 1996b) with slight modifications. MDCK cells were seeded at a density of 4.0×10^5 cells in 6-cm dishes and incubated for 24 h. Then, the cells were deprived of serum for 24 h. For the C3 treatment, the seeded cells were incubated first for 8 h, and then in the presence of various doses of C3 for 16 h. Next, the cells were deprived of serum for 24 h in the presence of C3. For some experiments, serum-deprived cells were treated with various doses of HA1077 or Y-32885 for 30 min. The cells were then incubated in DME containing 200 nM TPA or 50 pM HGF at 37°C for various periods. The TPA- or HGF-treated cells were treated with 10% (wt/vol) trichloroacetic acid. The resulting precipitates were subjected to immunoblotting with anti-pS854 Ab and anti-pnMBS Ab.

Subcellular Fractionation

MDCK cells were seeded at a density of 1.2×10^6 cells in 10-cm dishes. Non- and TPA-stimulated MDCK (5×10^7) cells were fractionated as described (Chen et al., 1992) with slight modifications. In brief, cells were washed and homogenized in buffer H (20 mM Hepes at pH 7.4, 5 mM KCl, 1 mM MgCl$_2$, 50 mM NaF, 30 mM sodium pyrophosphate, 20 μg/ml leupeptin, 50 μg/ml PMSF, 1 mM DTT, and 0.1 μM calyculin A) with dounce homogenizer. The homogenates were loaded onto 1 M sucrose in buffer H, and centrifuged at 1,600 g for 10 min. The precipitates contained nuclei. The supernatant fluids were further centrifuged at 100,000 g for 30 min. The resulting supernatants were used as cytoplasmic fraction. The resulting precipitates were used as membrane fraction. The precipitates containing nuclei were resuspended with 1 M sucrose in buffer H, and centrifuged at 1,600 g for 5 min. The resulting precipitates were used as nuclear fraction. We confirmed by phase contrast microscopy that nuclear fraction contained nearly the pure nuclei, and by immunoblot analysis of nuclear (CREB), cytoplasmic (Rho GDI), and membrane (E-cadherin) marker proteins that subcellular fractionation was successful (Montminy and Bilezikjian, 1987; Nagafuchi et al., 1987; Ueda et al., 1990).

Preparation of Interphase, Early Mitotic, and Later Stages of Cell Division Cells

MDCK cells in interphase, early mitotic (metaphase), and later stages of cell division cells were prepared as described (Bauer et al., 1998; Goto et al., 1998) with slight modifications. MDCK cells were seeded at a density of 1.2×10^6 cells in a 10-cm dish, and cultured for 24 h. Nocodazole was added directly to the medium at 0.33 μM, and then cells were cultured for additional 11 h. Mitotic cells were collected with PBS containing 4 mM EGTA and 0.33 μM nocodazole by mechanical shake off, and adherent cells were used as interphase cells. Mitotic cells were rinsed twice and suspended with nocodazole free medium, and plated onto the dishes. Cells at 0, 30, 60, or 90 min after removal of nocodazole were used as early mitotic and later stages of cell division cells. These cells were treated with 10% (wt/vol) trichloroacetic acid as described above.

Immunofluorescence Analysis

MDCK cells were fixed with 3.0% formaldehyde in PBS for 20 min and treated with PBS containing 0.2% Triton X-100 for 10 min on ice or acetone for 10 min at -20°C (for anti-pp2b Ab). REF52 cells were fixed with 3.0% formaldehyde in PBS for 10 min and treated with PBS containing 0.2% Triton X-100 for 10 min at room temperature. After being washed with PBS three times, the cells were incubated with anti-pS854 Ab, anti-pnMBS Ab, anti-pT558 Ab, anti-ERM Ab, anti-pp2b Ab, or anti-MLC Ab at 4°C overnight, TM71 for 2 h at room temperature, or anti-mMBS Ab for 1 h at room temperature. The cells were washed with PBS three times, then incubated with fluorescein isothiocyanate (FITC)-conjugated anti–rabbit or –mouse Ig Ab, Texas red–conjugated anti–rabbit, –mouse, or –rat Ig Ab for 1 h at room temperature or tetramethylrhodamine B isothiocyanate (TRITC)-phalloidin for 30 min at room temperature. DNAs were stained with 1 μg/ml of bisbenzimide Hoechst for 3 min at room temperature. Fluorescently labeled cells were examined with a Zeiss LSM510 (Carl Zeiss). In some experiments, fluorescent images (Figs. 4 and 5) were taken with PXL cooled CCD camera (Photometrics) with DeltaVision processing software (Applied Precision Inc.). Exposure time was adjusted to obtain FITC and Texas red or rhodamine images with roughly equal intensities in nonstimulated MDCK cells (see Fig. 4 A, a and b, and B, a and b, respectively; checked by histogram analysis). Under the same condition, the images of TPA- or HGF-stimulated MDCK cells were taken. The images of Figs. 4 A and 5 A, or Figs. 4 B and 5 B were treated with same establishment of contrast and brightness, respectively. Grayscale FITC and Texas red images were converted into green and red images, respectively, and then merged to synthesize RGB color images. A ratio image was created using an Image-Pro image processing system (Media Cybernetics). A grayscale image of anti-pS854 Ab was divided by a corresponding grayscale image of anti-mMBS Ab, and the resultant image was multiplied by 50.

Microinjection

REF52 cells were seeded at a density of 3×10^3 cells per 13-mm cover glass in 6-cm dishes and incubated for 48 h. MBP (5 mg/ml), C3 (0.1 mg/ml), C3 (0.1 mg/ml) plus GTPγS·RhoA^{141} (0.4 mg/ml), or MBP-RB/PH(TT) (5 mg/ml) was microinjected along with a marker protein (rabbit or mouse IgG at 1 mg/ml) into the cytoplasm of cells. After injection, the cells were incubated at 37°C for 30 min, and fixed as described above.

Results

Determination of the Sites of Phosphorylation of MBS by Rho-Kinase

We first determined the sites of phosphorylation of MBS by Rho-kinase in vitro as follows. Full-length MBS was expressed in *Spodoptera frugiperda* cells in a baculovirus system and purified. Purified MBS was then incubated with the GST-catalytic domain of Rho-kinase (GST-CAT; 6–553 aa). CAT has been previously shown to be constitutively active in vitro and in vivo (Amano et al., 1996a, 1997). Phosphorylated MBS was digested with *Achromobacter* protease I and subjected to high-performance liquid chro-

Peptide no.	Amino acid sequence*	Phosphorylated residues‡	Relative amount of phosphate in peptide§
			% total
AP-1	NASRIESLEQEK (residue 330–341)	Ser-332	3.4
AP-2	DTAGVIRSASSPRLSSSLDNK (residue 463–483)	Ser 472	8.5
AP-3	ARSRQARQSRRSTQGVTLTDLQEAEK (residue 685–710)	Ser-693, Ser-696, Thr-697	23.5
AP-4	RRSTGVSFWTQDSDENEQERQSDTEDGSSK (residue 852–881)	Ser-854, Thr-855	22.0
AP-5	TGSYGALAEITASKEAQK (residue 443–460)	Thr-443, Ser-445	6.0
AP-6	RDTQTDSVSRYDSSSTSSSDRYDSLLGRSASYSYLEERK (residue 882–920)	Thr-884, Ser-894, Ser-905	11.5
AP-7	ND		3.2
AP-8	YSRTYDETYARYRPVSTSSSSTPSSSSLSTLGSSLYASSQLNRPNSLVGITSAYSRGLTK (residue 759–818)	Thr-762, Ser-774	3.7

*Residue numbers correspond to Rat3 MBS.
‡The residues that showed the highest radioactivity in each peptide are underlined.
§Determined from radioactivity in the HPLC analysis as shown in Fig. 1. Total is not 100% because the amount of minor peaks is excluded.

matography. Two major (AP-3 and -4) and 6 minor (AP-1, -2 and -5–8) radioactive peptides were obtained (Fig. 1). As shown in Table I, we identified 14 phosphorylation sites of MBS by Rho-kinase. Thr-697 and Ser-854 turned out to be the major phosphorylation site in AP-3 and AP-4, respectively. When GST-MBS-NT (1–763 aa) or CT (758–1032 aa) was used as a substrate instead of full-length MBS, the essentially similar results were obtained (data not shown). Taking our previous studies and this result into consideration, the consensus sequence of Rho-kinase phosphorylation site is RXXS/T or RXS/T (Amano et al., 1996a; Goto et al., 1998; Matsui et al., 1998; Fukata et al., 1999). Rho-kinase seems to require the basic amino acid such as Arg close to its phosphorylation site. It has been previously reported that MBS is phosphorylated by protein kinase A (PKA), protein kinase C (PKC), and the endogenous kinase that is copurified with MBS from chicken gizzard (Ichikawa et al., 1996; Ito et al., 1997). MBS is phosphorylated at Thr-850 of Chicken M133, which corresponds to Thr-855 (one of the phosphorylation sites in AP-4) of Rat3 MBS, by PKA (Ito et al., 1997). The sites of phosphorylation of MBS by PKC are unknown. It should be noted that Thr-697 (a major phosphorylation site in AP-3) corresponds to Thr-695 of Chicken M133, has been shown to be phosphorylated by the endogenous kinase (Ichikawa et al., 1996). The phosphorylation of chicken MBS by the endogenous kinase results in inhibition of myosin phosphatase (Ichikawa et al., 1996). Thus, the phosphorylation of MBS at Thr-697 by Rho-kinase may result in inhibition of myosin phosphatase. The endogenous kinase has not been identified. However, the endogenous kinase appears to be distinct from Rho-kinase because some characters of the endogenous kinase are different from those of Rho-kinase (Amano, M., and K. Kaibuchi, unpublished data; Ichikawa et al., 1996).

Production and Characterization of the Site- and Phosphorylation State-specific Antibody for MBS

To investigate how the phosphorylation of MBS by Rho-

kinase is regulated in vivo, we prepared the site- and phosphorylation state-specific antibody for MBS. As shown in Table I, Rho-kinase phosphorylated multiple sites of MBS in vitro. Thr-697 was one of the major sites of phosphorylation of MBS by Rho-kinase in vitro. However, we can not distinguish the phosphorylation of Thr-697 by Rho-kinase and the endogenous kinase in vivo as described above. Ser-854, which was also one of the major sites of phosphorylation of MBS by Rho-kinase in vitro, is the phosphorylation site specific to Rho-kinase among known MBS kinases in vitro (We confirmed that PKC did not phosphorylate MBS at Ser-854: see below). The phosphorylation at Ser-854 can serve as a pertinent indicator to study MBS phosphorylation by Rho-kinase in vivo. Thus, we prepared the rabbit polyclonal antibody (anti-
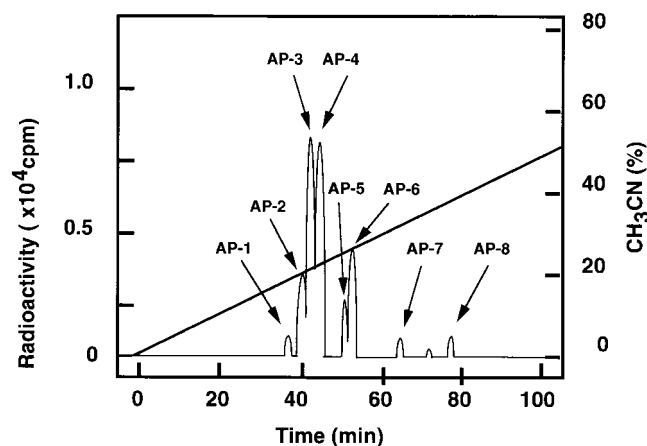

Figure 1. Determination of the sites of phosphorylation of MBS by Rho-kinase. Purified full-length MBS was incubated with GST-CAT in kinase buffer A containing 100 μM γ-[^{32}P]ATP for 1 h at 30°C, and the reaction product was digested with *Achromobacter* protease I. The obtained peptides were applied onto a C18 reverse phase column as described in Materials and Methods.
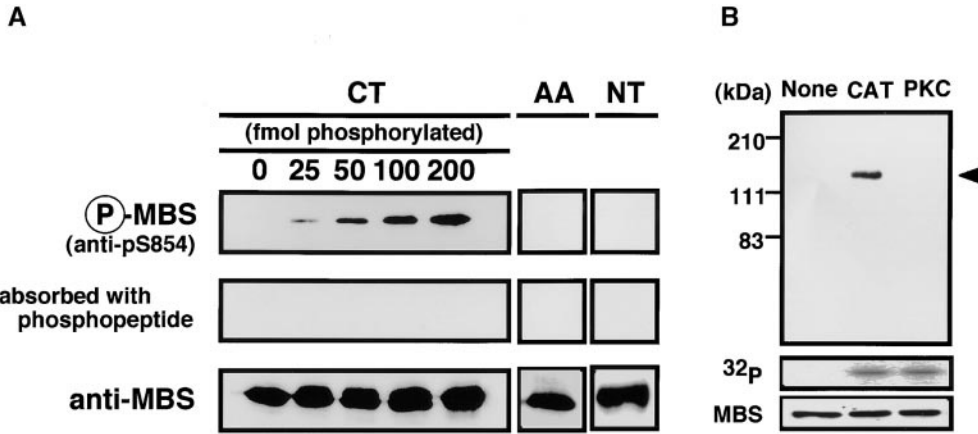
pS854 Ab), raised against the synthetic phosphopeptide (CEKRRphoshoS854TGVSF). The specificity of anti-pS854 Ab was examined by immunoblot analysis. Equal amounts of GST-MBS-CT with various ratios between phosphorylated and unphosphorylated forms were loaded on the gel. GST-MBS-CT phosphorylated by GST-CAT in vitro was specifically detected by anti-pS854 Ab in a dose-dependent manner (Fig. 2 A). The binding was neutralized by preincubation of the antibody with the antigen phosphopeptide. We also confirmed that anti-pS854 Ab recognized neither GST-MBS-CT[S854A, T855A] (substitution of residues by Ala), GST-MBS-NT phosphorylated by GST-CAT (Fig. 2 A) nor full-length MBS phosphorylated by PKC (Fig. 2 B). These results indicate that anti-pS854 Ab specifically recognizes MBS phosphorylated at Ser-854 by Rho-kinase.

Rho-Kinase–dependent Phosphorylation of MBS in MDCK Cells

Rho/Rho-kinase are implicated in HGF- and phorbol ester–induced membrane ruffling in MDCK and KB epithelial cells (Nishiyama et al., 1994; Takaishi et al., 1995; Fukata et al., 1999). We examined whether MBS was phosphorylated at Ser-854 via the Rho/Rho-kinase pathway in vivo. When total cell lysate of nonstimulated MDCK cells was immunoblotted with anti-pS854 Ab, MBS phosphorylated at Ser-854 was weakly detected. The addition of TPA enhanced the phosphorylation of MBS at Ser-854 (Fig. 3 A). Similar results were obtained when the cells were stimulated with HGF. A minor band with apparent relative molecular mass of 90 kD was also detected. This minor band may be a degradation product of MBS, because the immunoreactive band detected by anti-MBS Ab was found at the same position (data not shown). After TPA stimulation, the phosphorylation level of MBS at Ser-854 elevated within 3 min, reached maximum at ~30 min, and was sustained for at least 2 h (Fig. 3 B). The maximal phosphorylation level of MBS at Ser-854 was about fivefold the basal level. The stoichiometries of phosphory-

lation at Ser-854 were ~0.04 at the basal level and ~0.20 at the maximal level, respectively. Similar results were obtained when the cells were stimulated with HGF, although the level of MBS phosphorylation induced by HGF was slightly lower than that induced by TPA (Fig. 3 B). We also confirmed that the addition of dibutyryl cAMP did not induce the phosphorylation of MBS at Ser-854 (Fig. 3 A), whereas it induced the phosphorylation of cAMP-response element binding protein (CREB) at Ser-133 (data not shown). These results indicate that MBS is phosphorylated during the action of TPA and HGF in MDCK cells. We furthermore examined whether MBS was phosphorylated at Ser-854 via the Rho/Rho-kinase pathway during the action of TPA and HGF in MDCK cells (Fig. 3 C). *Botulinum* C3 ADP-ribosyltransferase (C3), which is thought to interfere with endogenous Rho functions, inhibited the focal adhesion formation in MDCK cells (~50% inhibition by incubation of 100 μg/ml of C3; data not shown). Under the conditions, the TPA-induced MBS phosphorylation was inhibited to a similar extent (Fig. 3 C). A similar inhibition was observed when the cells were pretreated with HA1077 or Y-32885, both of which are inhibitors of Rho-kinase (Fig. 3 C; Uehata et al., 1997).

Distribution of Phosphorylated MBS in MDCK Cells

We investigated the subcellular distribution of MBS phosphorylated at Ser-854 in MDCK cells. In the nonstimulated MDCK cells, the immunoreactivity of phosphorylated MBS was strong in the nucleus and diffuse in the cytoplasm, but not detected in cell–cell contact sites and free end of plasma membrane (Fig. 4 A, a). The TPA-induced membrane ruffling was detectable within 5 min and reached maximum at 15 min of exposure to TPA in the outer cell edge colonies (Nishiyama et al., 1994). Under the conditions, the addition of TPA enhanced the immunoreactivity of phosphorylated MBS in the cytoplasm, and the immunoreactivity of phosphorylated MBS was weakly detected in the membrane ruffling area (Fig. 4 A, c, arrowhead), where F-actin (Fig. 4 A, d, arrowhead),
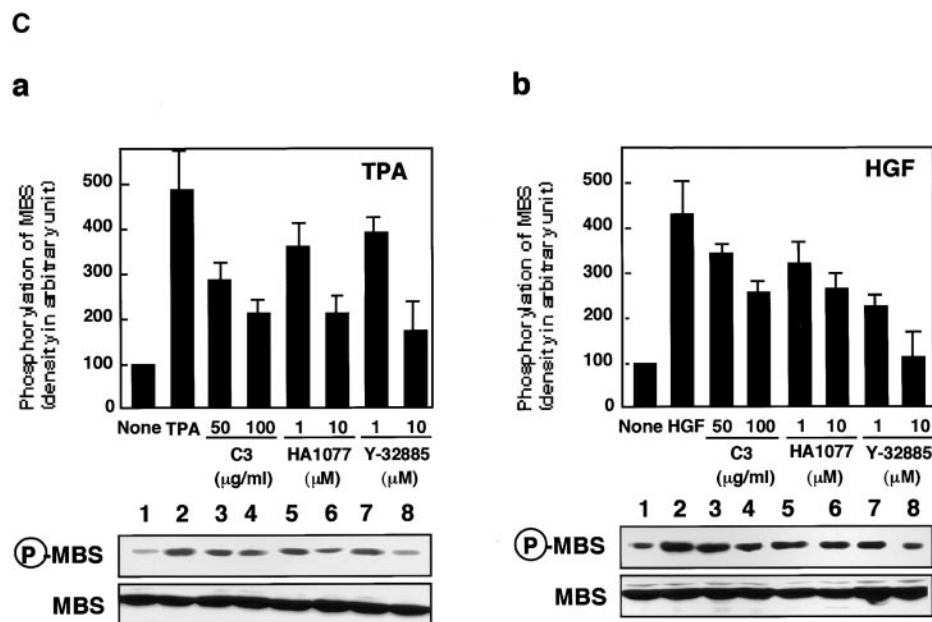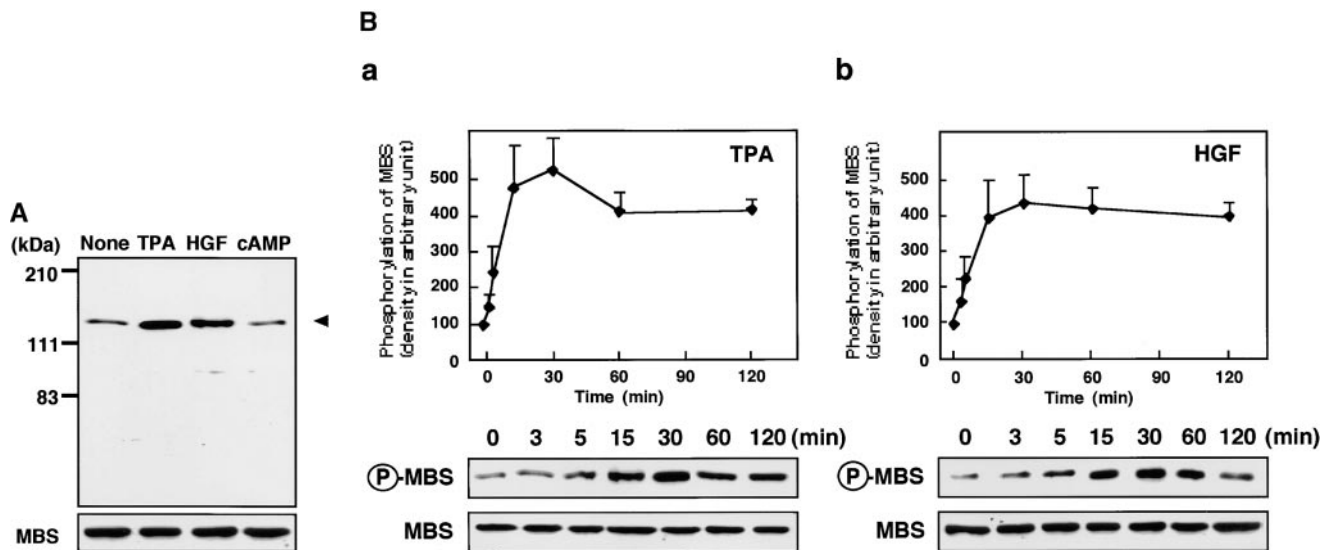
B

a

TPA

Phosphorylation of MBS (density in arbitrary unit)

Time (min)

0   3   5   15   30   60   120 (min)

(P)-MBS

MBS

b

HGF

Phosphorylation of MBS (density in arbitrary unit)

Time (min)

0   3   5   15   30   60   120 (min)

(P)-MBS

MBS

A

(kDa)   None   TPA   HGF   cAMP

210

111

83

MBS

C

a

TPA

Phosphorylation of MBS (density in arbitrary unit)

None TPA   50   100   1   10   1   10
              C3   HA1077   Y-32885
           (μg/ml)   (μM)   (μM)

1   2   3   4   5   6   7   8

(P)-MBS

MBS

b

HGF

Phosphorylation of MBS (density in arbitrary unit)

None HGF   50   100   1   10   1   10
              C3   HA1077   Y-32885
           (μg/ml)   (μM)   (μM)

1   2   3   4   5   6   7   8

(P)-MBS

MBS

Figure 3. Rho- and Rho-kinase–dependent phosphorylation of MBS at Ser-854 in MDCK cells. (A) TPA- and HGF-induced phosphorylation of MBS at Ser-854. Serum-deprived MDCK cells were stimulated with 200 nM TPA, 50 pM HGF for 15 min or 5 mM dibutyryl cAMP (cAMP) for 30 min, and the whole-cell lysates were resolved by SDS-PAGE followed by immunoblotting with anti-pS854 Ab (upper panel) and anti-pnMBS Ab (lower panel). Arrowhead indicates the position of MBS phosphorylated at Ser-854. A minor band with apparent relative molecular mass of 90 kD may be a degradation product of MBS. (B) Time course of the phosphorylation of MBS at Ser-854 in the TPA- and HGF-stimulated MDCK cells. Serum-deprived MDCK cells were stimulated with 200 nM TPA (a) or 50 pM HGF (b) for 3, 5, 15, 30, 60, or 120 min, and the whole-cell lysates were resolved by SDS-PAGE followed by immunoblotting with anti-pS854 Ab (upper panels) and anti-pnMBS Ab (lower panels). The amount of MBS phosphorylated at Ser-854 was quantitatively determined by scanning densitometry. The densities of the immunoreactive bands with anti-pS854 Ab were normalized by that of total MBS. The mean density of the immunoreactive bands with anti-pS854 Ab at 0 min was set at 100 arbitrary units. The values shown are means ± SE of triplicates. (C) Inhibition of the TPA- and HGF-induced MBS phosphorylation by C3 or Rho-kinase inhibitors. Nonpretreated (2), 50 or 100 μg/ml C3-pretreated (3 and 4), 1 or 10 μM of HA1077-pretreated (5 and 6), or 1 or 10 μM of Y-32885–pretreated (7 and 8) serum-deprived MDCK cells were stimulated with (2–8) or without (1) 200 nM TPA (a) or 50 pM HGF (b) for 15 min and the lysates were resolved by SDS-PAGE followed by immunoblotting with anti-pS854 Ab (upper panels) and anti-pnMBS Ab (lower panels). The densities of the immunoreactive bands with anti-pS854 Ab were normalized by that of total MBS. The mean density of the immunoreactive bands with anti-pS854 Ab in the nonstimulated cells was set at 100 arbitrary units. The values shown are means ± SE of triplicates.

MBS (Fukata et al., 1998) and phosphorylated α-adducin accumulated (Fukata et al., 1999). Similar results were obtained when the cells were stimulated with HGF instead of TPA (Fig. 4 A, e and f; arrowheads). The immunoreactivity of phosphorylated MBS in the nucleus, cytoplasm and membrane ruffling area was abolished by preincubation of the antibody with the antigen phosphopeptide (Fig. 4 A, g and h).

Next, we compared the distribution of phosphorylated

and total MBS. In nonstimulated MDCK cells, the immunoreactivity of total MBS was strong in the cytoplasm (Fig. 4 B, b; Inagaki et al., 1997). In TPA-stimulated MDCK cells, the immunoreactivity of total MBS was detected in the cytoplasm and the TPA-induced membrane ruffling area (Fig. 4 B, f; Fukata et al., 1998). The merged image of anti-pS854 Ab (green) and anti-MBS Ab (red) immunofluorescence enabled us to roughly estimate the phosphorylation state of MBS. Green, yellow, and red images

indicate high, intermediate, and low levels of phosphorylation of MBS at Ser-854, respectively. The merged image of phosphorylated and total MBS of the cytoplasm and free end of plasma membrane in the TPA-stimulated cells was more greenish than that of the cytoplasm in the nonstimulated cells (Fig. 4 B, c and g). Consistently, the ratio (phosphorylated MBS/MBS) was high in cytoplasm and membrane ruffling area of TPA-stimulated MDCK cells as compared with that of nonstimulated MDCK cells (Fig. 4 B, d and h). The ratio in nucleus was also increased by TPA stimulation. We found that phosphorylated MBS was more enriched in the membrane ruffling area as compared with Rho GDI, which is one of the cytoplasmic proteins (data not shown; Ueda et al., 1990). Similar results were obtained when the cells were stimulated with HGF instead of TPA (Fig. 4 B, k and l).

To further determine the subcellular distribution of phosphorylated MBS, we carried out the subcellular fractionation analysis (Fig. 4 C). Total MBS was detected mainly in cytoplasmic fractions in non- and TPA-stimulated MDCK cells. The amount of total MBS in each fractions of subcellular fractionation is consistent with the result of immunofluorescence study (Fig. 4, B and C). In nonstimulated MDCK cells, phosphorylated MBS was weakly detected in nuclear and cytoplasmic fractions. The addition of TPA increased phosphorylated MBS mainly in the cytoplasmic fraction and modestly in the nuclear fraction. In addition, phosphorylated MBS was weakly detected in membrane fraction. It should be also noted that although the immunoreactivity of phosphorylated MBS in immunofluorescence study was strong in the nucleus in the presence or absence of TPA (Fig. 4, A and B), the phosphorylation level of MBS in the nuclear fraction in the cells stimulated with TPA was lower than that in the cytoplasmic fraction in subcellular fractionation analysis (Fig. 4 C). This might be due to the rapid dephosphorylation of MBS during nuclear isolation. Severe dephosphorylation of MBS was not prevented during the subcellular fractionation under the present conditions. Therefore, the amount of phosphorylated MBS after subcellular fractionation may be less than that of phosphorylated MBS in intact cells. We found the additional band above phosphorylated MBS in nuclear fraction. We do not know exactly whether the additional band is an isoform of MBS or a nonspecific band. In fact, Shimizu et al. identified two isoforms of MBS (M130 and M133) from chicken gizzard (Shimizu et al., 1994). The similar isoforms may exist in MDCK cells. However, we could not rule out the possibility that pS854 Ab cross-reacted with other insoluble nuclear component in immunofluorescence study.

Distribution of Phosphorylated MBS in Migrating MDCK Cells

We compared the subcellular distribution of phosphorylated MBS with that of F-actin and phosphorylated MLC at Ser-19 in migrating MDCK cells. Between 2 and 16 h after the addition of TPA, the cells dissociated from each other and migrated, with polarized morphology and membrane ruffling in the leading edge. In the TPA-induced migrating cells, phosphorylated MBS was localized in the leading edge, where F-actin accumulated, and the poste-

rior region containing the nucleus (Fig. 5 A, a and b). Similar results were obtained as to the distribution of phosphorylated MLC in migrating MDCK cells (Fig. 5 A, c and d) as described (Matsumura et al., 1998). The merged image of phosphorylated and total MBS in the leading edge and the posterior region containing the nucleus in migrating MDCK cells was more greenish than that in the cytoplasm in the nonstimulated MDCK cells (Fig. 5 B, c and Fig. 4 B, c). Consistently, the ratio (phosphorylated MBS/MBS) was high in the leading edge and the posterior region containing the nucleus in migrating MDCK cells as compared with that in nonstimulated MDCK cells (Fig. 4 B, d and Fig. 5 B, d).

Colocalization of Phosphorylated MBS, F-Actin, and Phosphorylated MLC in REF52 Fibroblasts

We further investigated the subcellular distribution of phosphorylated MBS, F-actin, and phosphorylated MLC in REF52 fibroblasts. REF52 cells grown in 10% fetal bovine serum have thick actin stress fibers and vinculin-containing focal adhesions, and show a filamentous periodical pattern of myosin on stress fibers. We have previously shown that total MBS is localized on stress fibers (Inagaki, N., et al., 1997). Phosphorylated MBS was localized on stress fibers, cortical actin filaments, and in the nucleus in REF52 cells (Fig. 6 A, a). The double-immunostaining by TRITC-phalloidin and anti-pS854 Ab (Fig. 6 A, a and b) or anti-pp2b Ab (Fig. 6 A, c and d) demonstrated coexistence of phosphorylated MBS, F-actin and phosphorylated MLC on stress fibers and cortical actin filaments. The intracellular localization of phosphorylated MBS is consistent with in vitro binding of MBS and myosin (Alessi et al., 1992; Shimizu et al., 1994). There was the difference in localization of phosphorylated MBS between REF52 and MDCK cells. REF52 cells highly developed thick stress fibers (Fig. 6 A, b), whereas serum-starved MDCK cells had a few thin stress fibers (Fig. 4 A, b). Thus, phosphorylated MBS might not be detected in stress fibers in MDCK cells. Next, we compared the distribution of phosphorylated and total MBS. The distribution of phosphorylated MBS was similar to that of total MBS (Fig. 6 B, c). The ratio (phosphorylated MBS/MBS) image showed that the phosphorylation level of MBS was high on stress fiber and in nucleus (Fig. 6 B, d).

We examined the effects of C3 and dominant negative Rho-kinase [RB/PH(TT)] on the localization of phosphorylated MBS in REF52 cells (Fig. 6 C). C3 ADP-ribosylates Rho at Asn-41 and inactivates it, whereas RhoA[I41] is not ADP-ribosylated by C3 and is insensitive to C3. RB/PH(TT) (941–1388 aa) is composed of Rho-binding (RB) and pleckstrin-homology (PH) domains of Rho-kinase (Matsui et al., 1996). RB/PH(TT), which has point mutations in the RB domain and does not bind to Rho, interacts with the kinase domain of Rho-kinase and thereby inhibits the Rho-kinase activity without titrating out Rho in vitro (Amano et al., 1999). RB/PH(TT) functions as the dominant negative form of Rho-kinase in vivo (Amano et al., 1998). The microinjection of C3 into REF52 cells disrupted the stress fibers and decreased the phosphorylated MLC staining (Fig. 6 C, e and h) as described (Chihara et al., 1997). The filamentous pattern of phosphorylated
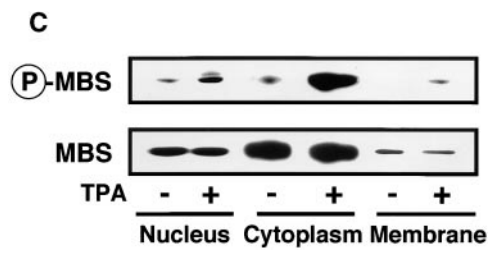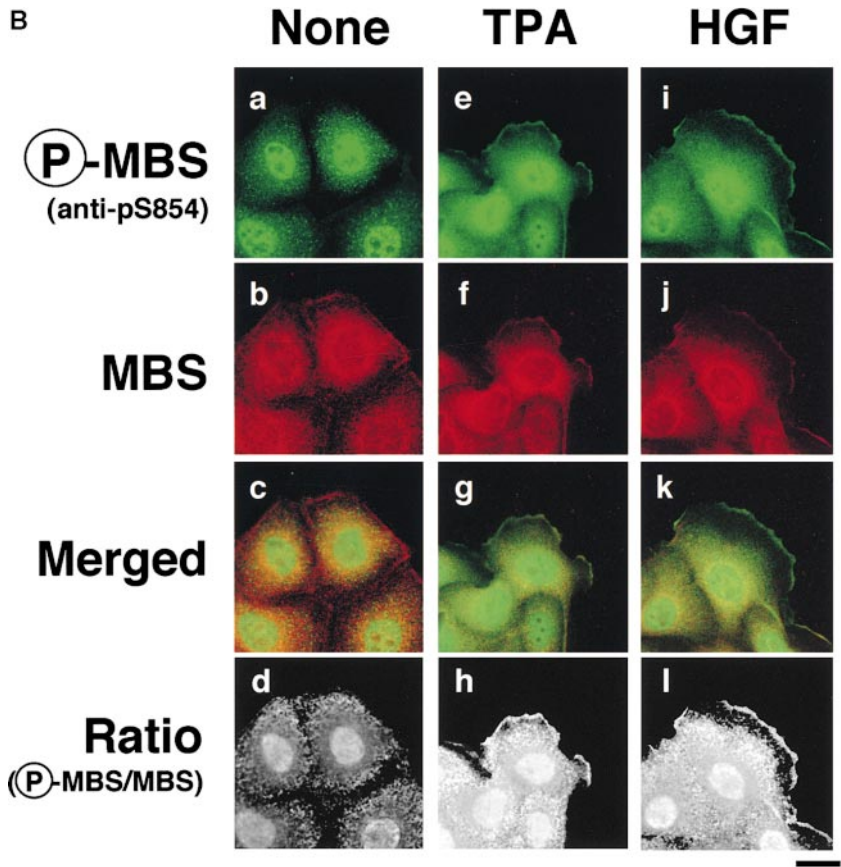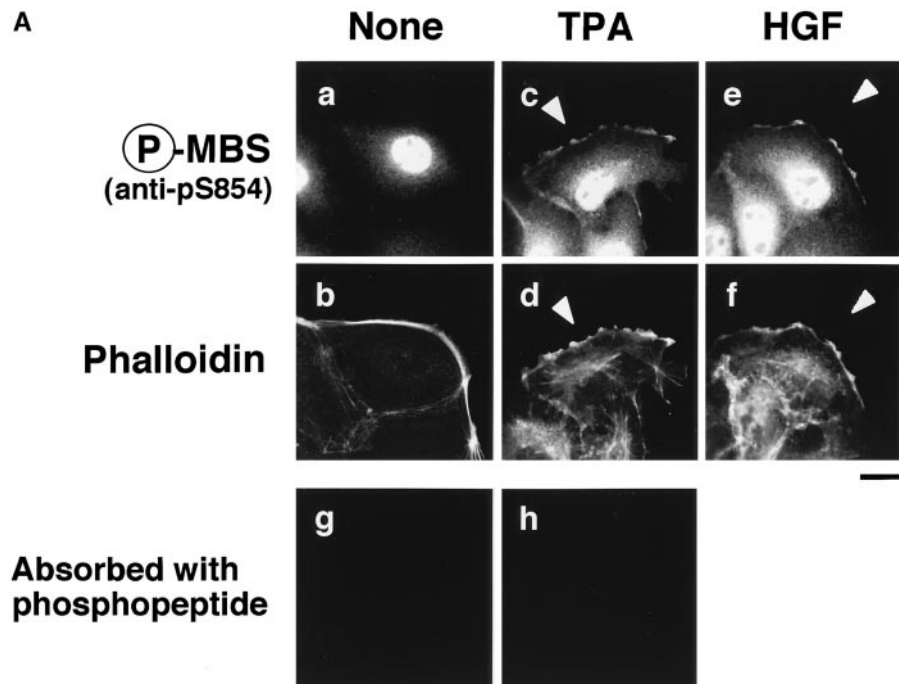
Figure 4. Distribution of Ser-854–phosphorylated MBS in the TPA- or HGF-stimulated MDCK cells. (A) Distribution of Ser-854–phosphorylated MBS. Serum-deprived MDCK cells were stimulated with 200 nM TPA (c, d, and h) or 50 pM HGF (e and f) for 15 min. MDCK cells were stained with anti-pS854 Ab (a, c, and e) or TRITC-phalloidin (b, d, and f). MDCK cells were also stained with anti-pS854 Ab absorbed with a 100-fold amount of antigen phosphopeptide (g and h). Arrowheads indicate the induced membrane ruffling. (B) Distribution of phosphorylated and total MBS. Serum-deprived MDCK cells were stimulated with 200 nM TPA (e–h) or 50 pM HGF (i–l) for 15 min. MDCK cells were doubly stained with anti-pS854 Ab (a, e, and i) and anti-mMBS Ab (b, f, and j). The merged (c, g, and k) and ratio (phosphorylated MBS/MBS; d, h, and l) images are shown. (C) Subcellular distribution of phosphorylated MBS. Non- (−) and TPA- (+) stimulated MDCK cells were separated into nuclear (nucleus), cytoplasmic (cytoplasm), and membrane (membrane) fractions, and the fractions were immunoblotted with anti-pS854 Ab (upper panel) and anti-pnMBS Ab (lower panel). These results are representative of three independent experiments. Bars, 10 μm.
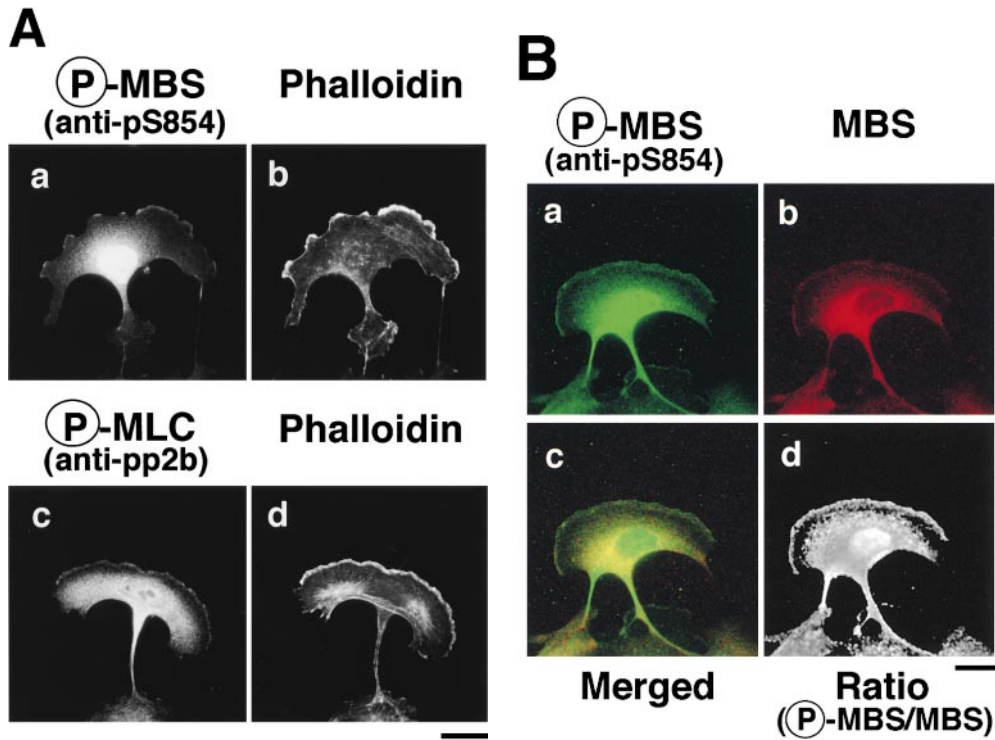
Figure 5. Distribution of phosphorylated MBS in migrating MDCK cells. (A) Serum-deprived MDCK cells were stimulated with 200 nM TPA for 2 h. Migrating MDCK cells were doubly stained with TRITC-phalloidin (b and d) and anti-pS854 Ab (a) or anti-pp2b Ab (c). (B) Localization of phosphorylated and total MBS in migrating MDCK cells. Migrating cells were doubly stained with anti-pS854 Ab (a) and anti-mMBS Ab (b). The merged (c) and ratio (phosphorylated MBS/MBS; d) images are shown. Bars, 10 μm.

MBS was also perturbed by the microinjection of C3 (Fig. 6 C, f). Under these conditions, total MBS and MLC were scattered in the cytoplasm (Fig. 6 C, g; Chihara et al., 1997). The coinjection of GTPγS·RhoA^{I41} with C3 reversed the effects of C3 (Fig. 6 B, i–l). The microinjection of RB/PH(TT) also disrupted the stress fibers (Fig. 6 C, m) and decreased the staining of phosphorylated MBS and MLC in REF52 cells (Fig. 6 C, n and p). Similar results were obtained when cells were treated with Rho-kinase inhibitors (HA1077 and Y-32885) (data not shown). It should be noted that the microinjection of C3 into REF52 decreased the staining of phalloidin in most cells, whereas that of RB/PH(TT) induced the disorganization of actin filaments (Fig. 6 C, m). C3 may induce depolymerization of F-actin through the inhibition of other Rho-targets such as p140mDia.

Distribution of Phosphorylated MBS and ERM Family Proteins during Cytokinesis

It has been shown that ERM family proteins and MLC phosphorylated at Ser-19 highly accumulate at the cleavage furrow during cytokinesis (Sato et al., 1991; Matsumura et al., 1998). In a recent study, we have found that Rho-kinase also highly and circumferentially accumulates at the cleavage furrow in various cell lines (Kosako et al., 1999), and that dominant negative Rho-kinase inhibits the progress of cytokinesis (Yasui et al., 1998). Here we examined the distribution of phosphorylated MBS during the different mitotic stages of MDCK cells. Phosphorylated MBS was enriched at the mid zone between the daughter chromosomes in late anaphase and at the cleavage furrow in telophase (Fig. 7 A, a and b). Phosphorylated MBS persisted at the mid body until the end of cytokinesis (Fig. 7

A, c). Next, we compared the distribution of phosphorylated MLC and ERM family proteins to that of phosphorylated MBS during different mitotic stages of MDCK cells. The staining patterns of phosphorylated MLC were spatially and temporally similar to that of phosphorylated MBS in dividing cells (Fig. 7 A, g–i). Phosphorylated ERM family proteins accumulated in the microvilli-like structures in the cell body at all stages as described (Oshiro et al., 1998), and highly and circumferentially accumulated around the mid zone in late anaphase, and the cleavage furrow in telophase. The staining patterns of phosphorylated ERM family proteins were also similar to that of phosphorylated MBS, but phosphorylated ERM family proteins did not persist at the mid body until the end of cytokinesis (Fig. 7 A, m–o). Vimentin is the most widely expressed intermediate filament protein, which is phosphorylated by Rho-kinase at Ser-71 (Goto et al., 1998). Using TM71, which recognizes the phosphorylation of vimentin at Ser-71, vimentin is shown to be specifically phosphorylated at the cleavage furrow whereas total vimentin is diffusely localized throughout the cytoplasm (Yasui et al., 1998). Although phosphorylated vimentin, MBS and ERM family proteins accumulated around the cleavage furrow, they were not completely colocalized (Fig. 7 B, f and l). Phosphorylated adducin, which is one of the Rho-kinase substrates, was diffusely localized throughout the cytoplasm (Fig. 7 B, m). It should be noted that total MBS was diffusely localized throughout the cytoplasm, but not accumulated at the cleavage furrow (Fig. 7 B, a). In contrast, phosphorylated MBS strongly accumulated at the cleavage furrow (Fig. 7 B, d), indicating that MBS was phosphorylated specifically at the cleavage furrow. Total ERM family proteins was diffusely localized throughout the cytoplasm, and at the microvilli and cleavage furrow
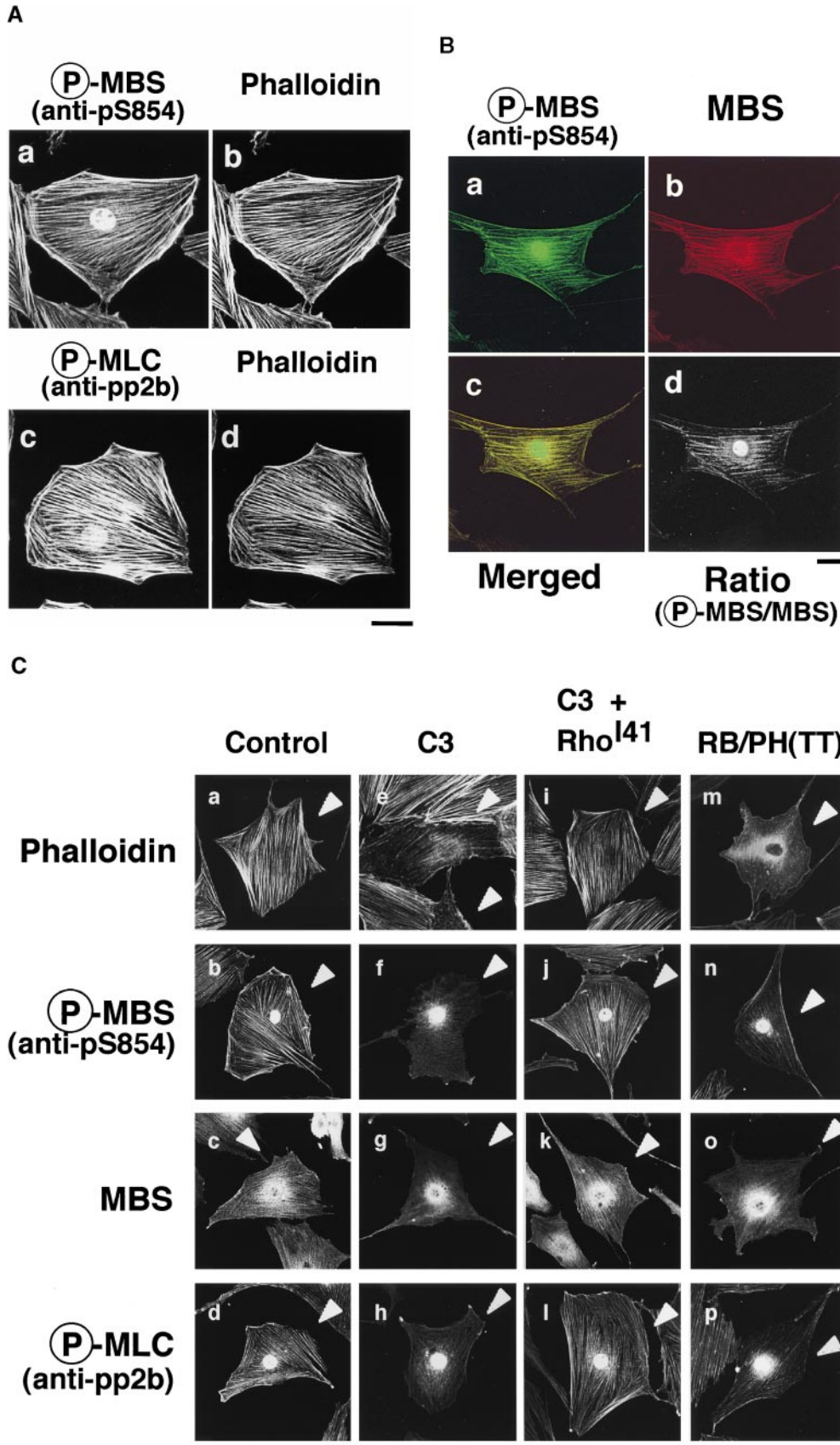
Figure 6. Colocalization of phosphorylated MBS, F-actin and phosphorylated MLC in REF52 fibroblasts. (A) Localization of phosphorylated MBS. REF52 cells were doubly stained with TRITC-phalloidin (b and d) and anti-pS854 Ab (a) or anti-pp2b Ab (c). (B) Distribution of phosphorylated and total MBS in REF52 cells. REF52 cells were doubly stained with anti-pS854 Ab (a) and anti-mMBS Ab (b). The merged (c) and ratio (phosphorylated MBS/MBS; d) images are shown. (C) Inhibition of phosphorylation of MBS by C3 or dominant negative Rho-kinase. REF52 cells were microinjected with MBP (5.0 mg/ml) (a–d), C3 (0.1 mg/ml) (e–h), C3 plus GTPγS·RhoA^I41 (0.4 mg/ml) (i–l), or MBP-RB/PH(TT) (5.0 mg/ml) (m–p). REF52 cells were stained with TRITC-phalloidin (a, e, i, and m), anti-pS854 Ab (b, f, j, and n), anti-pnMBS Ab (c, g, k, and o), and anti-pp2b Ab (d, h, l, and p). The arrowheads indicate the injected cells. Bars, 10 μm.
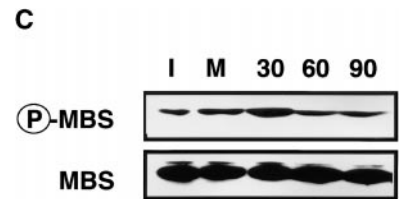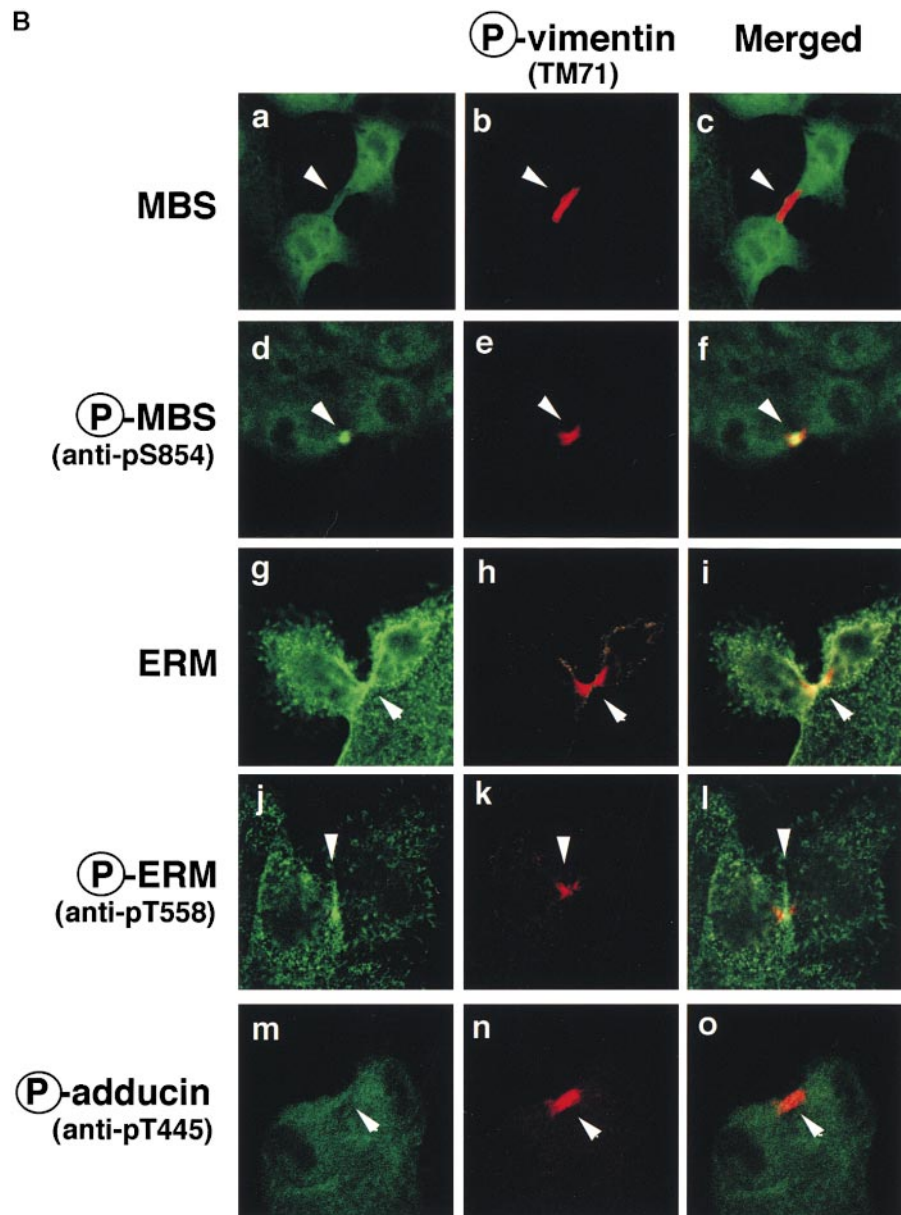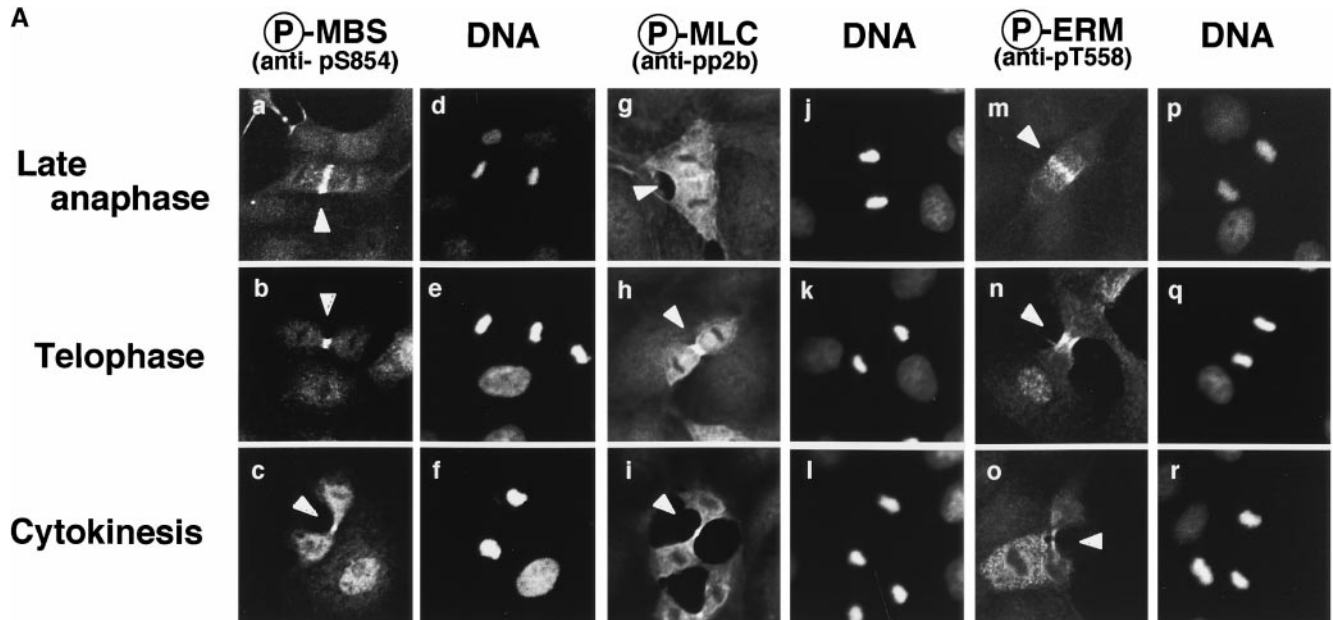
Figure 7. Distribution of phosphorylated MBS and ERM family proteins during cytokinesis in MDCK cells. (A) Accumulation of phosphorylated MBS and ERM family proteins at the cleavage furrow. MDCK cells in late anaphase (a, d, g, j, m, and p), telophase (b, e, h, k, n, and q) or cytokinesis (c, f, i, l, o, and r; indicated by arrowheads) stained with anti-pS854 Ab (a–c), anti-pp2b Ab (g–i), or anti-pT558 Ab (m–o) are shown. DNAs were stained with bisbenzimide Hoechst (d–f, j–l, and p–r). (B) Specific localization of phosphorylated Rho-kinase substrates during cytokinesis. MDCK cells in cytokinesis doubly stained with TM71 (b, e, h, k, and n) and anti-pnMBS Ab (a), anti-pS854 Ab (d), anti-ERM Ab (g), anti-pT558 Ab (j), and anti-pT445 Ab (m). Merged images are shown (c, f, i, l, and o). (C) Elevation of phosphorylation of MBS at Ser-854 during cytokinesis. Total cell lysates were prepared from interphase cells (I), early mitotic cells (metaphase, M) and cells at different stages of cell division (time in minutes after the release of mitotic arrest), and immunoblotted with anti-pS854 Ab (upper panel) or anti-pnMBS Ab (lower panel). These results are representative of three independent experiments. Bars, 10 μm.

(Fig. 7 B, g), whereas phosphorylated ERM family proteins accumulated at the microvilli and cleavage furrow preferentially (Fig. 7 B, j). To further confirm that the phosphorylation level of MBS at Ser-854 elevates during the cytokinesis, immunoblot analysis of synchronized MDCK cells lysates was carried out (Fig. 7 C). By release from mitotic arrest by nocodazole, early mitotic cells synchronistically entered into later stages of cell division, and at 30 min after release of mitotic arrest, ~40% of the cells were in late anaphase, telophase or cytokinesis. At later phases, the cells were in post mitotic spreading (60–180 min) as described (data not shown; Matsumura et al., 1998). The immunoreactivity of anti-pS854 Ab was increased at 30 min after release of mitotic arrest as compared with that in interphase and early mitotic cells (Fig. 7 C). This increment of phosphorylation level of MBS was reversed at 60 min.

Discussion

Phosphorylation of MBS by Rho-Kinase In Vitro

Here we identified Ser-854 as one of the major sites of phosphorylation of MBS by Rho-kinase in vitro, and prepared a rabbit polyclonal antibody (anti-pS854 Ab), raised against the synthetic phosphopeptide. Anti-pS854 Ab specifically recognized MBS phosphorylated by Rho-kinase, but not by PKC in vitro. Since Ser-854 in MBS is the phosphorylation site specific to Rho-kinase among known MBS kinases, the phosphorylation of MBS at Ser-854 appears to be a useful indicator of the Rho/Rho-kinase activation in vivo. We found that Thr-697 was also one of the major sites of phosphorylation of MBS by Rho-kinase in vitro. We have previously reported that the phosphatase activity toward MLC is inhibited when MBS is phosphorylated by Rho-kinase (Kimura et al., 1996). The endogenous kinase that is copurified with MBS from chicken gizzard (Ichikawa et al., 1996), phosphorylates MBS at Thr-695 (M133), which corresponds to Thr-697 of Rat3 MBS, and thereby inactivates the phosphate activity (Ichikawa et al., 1996). The phosphorylation of MBS at Thr-697 by Rho-kinase may result in inhibition of myosin phosphatase. The endogenous kinase appears to be distinct from Rho-kinase because the endogenous kinase is not inhibited by H7, which is one of the PKC inhibitors, whereas Rho-kinase is inhibited by H7 (unpublished data), and because the endogenous kinase but not Rho-kinase phosphorylates MLC at PKC sites (Amano et al., 1996a; Ichikawa et al., 1996). Since several sites of MBS including Thr-697 and Ser-854 were phosphorylated by Rho-kinase in vitro, further studies are necessary to determine which sites are the major sites of phosphorylation of MBS by Rho-kinase in vivo, and which phosphorylation sites are responsible for the inhibition of the phosphatase activity by Rho-kinase in vitro and in vivo.

Phosphorylation of MBS by Rho-Kinase In Vivo

We have previously shown that expression of dominant active Rho in NIH 3T3 cells results in an increment of MBS phosphorylation (Kimura et al., 1996). MBS is phos-
phorylated and the myosin phosphatase activity is inactivated during the action of thromboxane A_2 in platelets, and both reactions are inhibited by a prior treatment of platelets with C3 (Nakai et al., 1997). Similar observations are obtained in endothelial cells during the action of thrombin (Essler et al., 1998). Here we found by use of anti-pS854 Ab that the stimulation of MDCK cells with TPA or HGF induced the phosphorylation of MBS at Ser-854, and that pretreatment of the cells with C3 or Rho-kinase inhibitors inhibited the TPA- or HGF-induced MBS phosphorylation. It is possible that TPA induced the phosphorylation of MBS at Ser-854 through direct phosphorylation by PKC. However, this possibility is unlikely because anti-pS854 Ab did not recognize MBS phosphorylated by PKC in vitro. Phosphorylated MBS accumulated on stress fibers in REF52 cells. The microinjection of C3 or dominant negative Rho-kinase into REF52 cells weakened the accumulation of phosphorylated MBS. These results indicate that MBS is phosphorylated by Rho-kinase downstream of Rho in non-muscle cells. Myosin phosphatase binds to phosphorylated Rho-kinase substrates such as MLC via MBS and dephosphorylates them. Rho-kinase phosphorylates MBS, which leads to the inactivation of myosin phosphatase in vitro (Kimura et al., 1996, 1998; Fukata et al., 1998). Taken together, these observations suggest that the phosphorylation of MBS by Rho-kinase is involved in regulating the phosphorylation level of Rho-kinase substrates in non-muscle cells.

Evidence is accumulating that Rho regulates the phosphorylation level of MLC through Rho-kinase and myosin phosphatase in smooth muscle cells (Hirata et al., 1992; Noda et al., 1995; Gong et al., 1996; Kureishi et al., 1997). Because contraction of smooth muscle cells determines the size of lumen in blood vessels, airways, the gastrointestinal tract, uterus, and bladder, abnormal contraction can cause diseases such as hypertension and asthma (Somlyo, 1997). It has recently been shown that Y-27632 (one of the specific inhibitors for Rho-kinase) selectively inhibits smooth muscle contraction and corrects blood pressure in several hypertensive rat models (Uehata et al., 1997). Thus, the Rho-kinase–mediated pathway appears to be involved in the pathogenesis of hypertension. Phosphorylation of MBS by Rho-kinase may play an important role in generating a certain types of abnormal contraction of smooth muscle. In this regard, we have recently found that Rho-kinase phosphorylates MBS at Ser-854 during porcine coronary artery spasm (Kandabashi et al., 1999).

Phosphorylation of MBS in Motile Cells

Membrane ruffling is observed in the leading edges of motile cells and is thought to be essential for cell motility (Cooper, 1991). A force arising from actin polymerization appears to drive lamellipodial protrusion (Mitchison and Cramer, 1996), which is thought to be regulated by the small GTPase Rac (Ridley et al., 1992; Hall, 1998). Actin in the membrane ruffling area is thought to be continuously depolymerized and then repolymerized during cell movement (Mitchison and Cramer, 1996). A force derived from myosin II driven by MLC phosphorylation, which is thought to be regulated by Rho (Amano et al., 1996a, 1998) in the membrane ruffling area and posterior region

of motile cells may also contribute to cell movement (Lauffenburger et al., 1996; Mitchison and Cramer, 1996). Indeed, injection of anti–MLC-kinase Ab diminishes the cell motility of macrophages (Wilson et al., 1991). Moreover, Matsumura et al. (1998) have recently shown that the phosphorylation level of MLC is high in the leading edge and posterior region containing the nucleus during the cell migration. It has been previously reported that the addition of TPA decreases force that the whole cell applies to the substrate in certain migrating fibroblasts (Danowski and Harris, 1988). The cycling between phosphorylated and nonphosphorylated states of MLC may be necessary for cell migration. In this regard, we have recently reported that microinjection of either dominant negative or constitutively active Rho-kinase inhibits cell migration of NRK cells (Fukata et al., 1999).

We have recently found that the microinjection of dominant negative Rho-kinase inhibits the TPA- or HGF-induced membrane ruffling in MDCK cells, indicating that Rho-kinase is necessary for the cell motility (Fukata et al., 1999). Here we found that MBS phosphorylated at Ser-854 as well as MLC phosphorylated at Ser-19 were localized in the leading edge and posterior region in migrating MDCK cells. We have recently found that phosphorylated α-adducin accumulates in the leading edge in migrating MDCK cells (Fukata et al., 1999). Myosin phosphatase interacts with both MLC and adducin through MBS, and dephosphorylates the phosphorylated MLC and α-adducin (Kimura et al., 1996, 1998). Taken together, the above observations suggest that myosin phosphatase and Rho-kinase cooperatively regulate the MLC phosphorylation in the leading edge and posterior region in migrating MDCK cells, and the α-adducin phosphorylation in the leading edge.

Phosphorylation of MBS in Fibroblasts

Rho-kinase is thought to regulate the formation of actin stress fibers (Leung et al., 1996; Amano et al., 1997; Ishizaki et al., 1997). We have recently found that the expression of mutant $MLC^{T18D, S19D}$ (substitution of residues by Asp), which is known to lead to the activation of myosin ATPase and a conformational change of myosin II when reconstituted with myosin heavy chain in vitro (Kamisoyama et al., 1994; Sweeney et al., 1994; Bresnick et al., 1995), also enhances the formation of stress fiber (Amano et al., 1998). Thus, it is likely that the Rho/Rho-kinase pathway plays a critical role in the formation of stress fiber through myosin II activation. Here we found that phosphorylated MBS was localized on stress fibers in REF52 cells. The microinjection of C3 or dominant negative Rho-kinase into REF52 cells disrupted stress fibers and weakened the accumulation of phosphorylated MBS. These observations suggest that myosin phosphatase and Rho-kinase cooperatively regulate the MLC phosphorylation in fibroblasts, which in turn induce the formation of stress fiber.

Phosphorylation of MBS during Cytokinesis

Rho, Rho-kinase, and ERM family proteins accumulate at the cleavage furrow (Sato et al., 1991; Takaishi et al., 1995; Kosako et al., 1999), where MLC phosphorylation occurs (Matsumura et al., 1998). The expression of C3 or dominant negative Rho-kinase inhibits cytokinesis, resulting in multiple nuclei (Kishi et al., 1993; Mabuchi et al., 1993; Yasui et al., 1998). Thus, MLC phosphorylation by the Rho/Rho-kinase pathway appears to provide contractility to the contractile ring and to play a critical role in cytokinesis. Rho-kinase also phosphorylates intermediate filament proteins such as glial fibrillary acidic protein (GFAP) and vimentin, exclusively at the cleavage furrow during cytokinesis (Kosako et al., 1997; Goto et al., 1998). The expression of GFAP mutated at Rho-kinase phosphorylation sites induces impaired segregation of glial filament into postmitotic daughter cells (Yasui et al., 1998). Thus, Rho-kinase appears to be essential not only for cytokinesis but also for the segregation of GFAP filaments into daughter cells which in turn ensures efficient cellular separation. Here we found that phosphorylated MBS as well as phosphorylated ERM family proteins accumulated at the cleavage furrow, where phosphorylated MLC and vimentin accumulated. Indeed, the phosphorylation level of MBS elevated during cytokinesis. Taken together, these results suggest that myosin phosphatase spatiotemporally regulates the phosphorylation state of certain substrates including MLC and ERM family proteins during cytokinesis in cooperation with Rho-kinase under the control of Rho. Recently, it has been shown that citron kinase, another Rho-binding kinase with structural similarity in the kinase domain to Rho-kinase, accumulates at the cleavage furrow and may play an important role in the contractile process during cytokinesis (Madaule et al., 1998). Further analysis of different and redundant functions of both Rho-binding kinases will help us to elucidate the molecular mechanism underlying cytokinesis downstream of Rho.

References

Alessi, D., L.K. MacDougall, M.M. Sola, M. Ikebe, and P. Cohen. 1992. The control of protein phosphatase-1 by targeting subunits. The major myosin phosphatase in avian smooth muscle is a novel form of protein phosphatase-1. *Eur. J. Biochem.* 210:1023–1035.

Amano, M., M. Ito, K. Kimura, Y. Fukata, K. Chihara, T. Nakano, Y. Matsuura, and K. Kaibuchi. 1996a. Phosphorylation and activation of myosin by Rho-associated kinase (Rho-kinase). *J. Biol. Chem.* 271:20246–20249.

Amano, M., H. Mukai, Y. Ono, K. Chihara, T. Matsui, Y. Hamajima, K. Okawa, A. Iwamatsu, and K. Kaibuchi. 1996b. Identification of a putative target for Rho as a serine-threonine kinase, PKN. *Science.* 271:648–650.

Amano, M., K. Chihara, K. Kimura, Y. Fukata, N. Nakamura, Y. Matsuura, and K. Kaibucni. 1997. Formation of actin stress fibers and focal adhesions enhanced by Rho-kinase. *Science.* 275:1308–1311.

Amano, M., K. Chihara, N. Nakamura, Y. Fukata, T. Yano, M. Shibata, M. Ikebe, and K. Kaibuchi. 1998. Myosin II activation promotes neurite retraction during the action of Rho and Rho-kinase. *Genes Cells.* 3:177–188.

Amano, M., K. Chihara, N. Nakamura, T. Kaneko, Y. Matsuura, and Kozo Kaibuchi. 1999. The COOH terminus of Rho-kinase negatively regulates Rho-kinase activity. *J. Biol. Chem.* 274:32418–32424.

Bauer, A., H. Lickert, R. Kemler, and J. Stappert. 1998. Modification of the E-cadherin-catenin complex in mitotic Madin-Darby canine kidney epithelial cells. *J. Biol. Chem.* 273:28314–28321.

Bresnick, A.R., V.L. Wolff-Long, O. Baumann, and T.D. Pollard. 1995. Phosphorylation on threonine-18 of the regulatory light chain dissociates the ATPase and motor properties of smooth muscle myosin II. *Biochemistry.* 34: 12576–12583.

Cachero, T.G., A.D. Morielli, and E.G. Peralta. 1998. The small GTP-binding protein RhoA regulates a delayed rectifier potassium channel. *Cell.* 93:1077–1085.

Chen, R.H., C. Sarnecki, and J. Blenis. 1992. Nuclear localization and regulation of erk- and rsk-encoded protein kinases. *Mol. Cell Biol.* 12:915–927.

Chihara, K., M. Amano, N. Nakamura, T. Yano, M. Shibata, T. Tokui, H. Ichikawa, R. Ikebe, M. Ikebe, and K. Kaibuchi. 1997. Cytoskeletal rearrangements and transcriptional activation of *c-fos* serum response element by Rho-kinase. *J. Biol. Chem.* 272:25121–25127.

Cooper, J.A. 1991. The role of actin polymerization in cell motility. *Annu. Rev. Physiol.* 53:585–605.

Danowski, B.A., and A.K. Harris. 1988. Changes in fibroblast contractility, morphology, and adhesion in response to a phorbol ester tumor promoter. *Exp. Cell Res.* 177:47–59.

Essler, M., M. Amano, H.J. Kruse, K. Kaibuchi, P.C. Weber, and M. Aepfelbacher. 1998. Thrombin inactivates myosin light chain phosphatase via Rho and its target Rho kinase in human endothelial cells. *J. Biol. Chem.* 272: 21867–21874.

Fukata, Y., K. Kimura, N. Oshiro, H. Saya, Y. Matsuura, and K. Kaibuchi. 1998. Association of the myosin-binding subunit of myosin phosphatase and moesin: dual regulation of moesin phosphorylation by Rho-associated kinase and myosin phosphatase. *J. Cell Biol.* 141:409–418.

Fukata, Y., N. Oshiro, N. Kinoshita, Y. Kawano, Y. Matsuoka, V. Bennett, Y. Matsuura, and K. Kaibuchi. 1999. Phosphorylation of adducin by Rho-kinase plays a crucial role in cell motility. *J. Cell Biol.* 145:347–361.

Gong, M.C., K. Iizuka, G. Nixon, J.P. Browne, A. Hall, J.F. Eccleston, M. Sugai, S. Kobayashi, A.V. Somlyo, and A.P. Somlyo. 1996. Role of guanine nucleotide-binding proteins--ras-family or trimeric proteins or both-in Ca^{2+} sensitization of smooth muscle. 1996. *Proc. Natl. Acad. Sci. USA.* 93:1340–1345.

Goto, H., H. Kosako, K. Tanabe, M. Yanagida, M. Sakurai, M. Amano, K. Kaibuchi, and M. Inagaki. 1998. Phosphorylation of vimentin by Rho-associated kinase at a unique amino-terminal site that is specifically phosphorylated during cytokinesis. *J. Biol. Chem.* 273:11728–11736.

Hall, A. 1998. Rho GTPases and the actin cytoskeleton. *Science.* 279:509–514.

Hartshorne, D.J., M. Ito, and F. Erdodi. 1998. Myosin light chain phosphatase: subunit composition, interactions and regulation. *J. Muscle Res. Cell Motil.* 19:325–341.

Hill, C.S., J. Wynne, and R. Treisman. 1995. The Rho family GTPases RhoA, Rac1, and Cdc42Hs regulate transcriptional activation by SRF. *Cell.* 81: 1159–1170.

Hirata, K., A. Kikuchi, T. Sasaki, S. Kuroda, K. Kaibuchi, Y. Matsuura, H. Seki, K. Saida, and Y. Takai. 1992. Involvement of rho p21 in the GTP-enhanced calcium ion sensitivity of smooth muscle contraction. *J. Biol. Chem.* 267:8719–8722.

Hirose, M., T. Ishizaki, N. Watanabe, M. Uehata, O. Kranenburg, W.H. Moolenaar, F. Matsumura, M. Maekawa, H. Bito, and S. Narumiya. 1998. Molecular dissection of the Rho-associated protein kinase (p160ROCK)-regulated neurite remodeling in neuroblastoma N1E-115 cells. *J. Cell Biol.* 141:1625–1636.

Ichikawa, K., M. Ito, and D.J. Hartshorne. 1996. Phosphorylation of the large subunit of myosin phosphatase and inhibition of phosphatase activity. *J. Biol. Chem.* 271:4733–4740.

Inagaki, M., N. Inagaki, T. Takahashi, and Y. Takai. 1997. Phosphorylation-dependent control of structures of intermediate filaments: a novel approach using site- and phosphorylation state-specific antibodies. *J. Biochem.* 121:407–414.

Inagaki, N., M. Nishizawa, M. Ito, M. Fujioka, T. Nakano, S. Tsujino, K. Matsuzawa, K. Kimura, K. Kaibuchi, and M. Inagaki. 1997. Myosin binding subunit of smooth muscle myosin phosphatase at the cell-cell adhesion sites in MDCK cells. *Biochem. Biophys. Res. Commun.* 230:552–556.

Ishizaki, T., M. Maekawa, K. Fujisawa, K. Okawa, A. Iwamatsu, A. Fujita, N. Watanabe, Y. Saito, A. Kakizuka, N. Morii, and S. Narumiya. 1996. The small GTP-binding protein Rho binds to and activates a 160 kDa Ser/Thr protein kinase homologous to myotonic dystrophy kinase. *EMBO (Eur. Mol. Biol. Organ.) J.* 15:1885–1893.

Ishizaki, T., M. Naito, K. Fujisawa, M. Maekawa, N. Watanabe, Y. Saito, and S. Narumiya. 1997. p160ROCK, a Rho-associated coiled-coil forming protein kinase, works downstream of Rho and induces focal adhesions. *FEBS Lett.* 404:118–124.

Ito, M., J. Feng, S. Tsujino, N. Inagaki, M. Inagaki, J. Tanaka, K. Ichikawa, D.J. Hartshorne, and T. Nakano. 1997. Interaction of smooth muscle myosin phosphatase with phospholipids. *Biochemistry.* 36:7607–7614.

Jalink, K., E.J. van Corven, T. Hengeveld, N. Morii, S. Narumiya, and W.H. Moolenaar. 1994. Inhibition of lysophosphatidate- and thrombin-induced neurite retraction and neuronal cell rounding by ADP ribosylation of the small GTP-binding protein Rho. *J. Cell Biol.* 126:801–810.

Johnson, D., P. Cohen, M.X. Chen, Y.H. Chen, and P.T. Cohen. 1997. Identification of the regions on the M110 subunit of protein phosphatase 1M that interact with the M21 subunit and with myosin. *Eur. J. Biochem.* 244:931–993.

Kaibuchi, K., S. Kuroda, and M. Amano. 1999. Regulation of the cytoskeleton and cell adhesion by the Rho family GTPases in mammalian cells. *Annu. Rev. Biochem.* 68:459–486.

Kamisoyama, H., Y. Araki, and M. Ikebe. 1994. Mutagenesis of the phosphorylation site (serine 19) of smooth muscle myosin regulatory light chain and its effects on the properties of myosin. *Biochemistry.* 33:840–847.

Kandabashi, T., H. Shimokawa, K. Miyata, I. Kunihiro, Y. Kawano, Y. Fukata, T. Higo, K. Egashira, S. Takahasi, K. Kaibuchi, and A. Takeshita. 1999. Inhibition of myosin phosphatase by up-regulated Rho-kinase plays a key role for coronary artery spasm in a porcine model with interleukin-1β. *Circulation.* In press.

Katoh, H., J. Aoki, A. Ichikawa, and M. Negishi. 1998. p160 RhoA-binding kinase ROKα induces neurite retraction. *J. Biol. Chem.* 273:2489–2492.

Kimura, K., M. Ito, M. Amano, K. Chihara, Y. Fukata, M. Nakafuku, B. Yamamori, J. Feng, T. Nakano, K. Okawa, et al. 1996. Regulation of myosin phosphatase by Rho and Rho-associated kinase (Rho-kinase). *Science.* 273: 245–248.

Kimura, K., Y. Fukata, Y. Matsuoka, V. Bennett, Y. Matsuura, K. Okawa, A. Iwamatsu, and K. Kaibuchi. 1998. Regulation of the association of adducin with actin filaments by Rho-associated kinase (Rho-kinase) and myosin phosphatase. *J. Biol. Chem.* 273:5542–5548.

Kishi, K., T. Sasaki, S. Kuroda, T. Itoh, and Y. Takai. 1993. Regulation of cytoplasmic division of *Xenopus* embryo by rho p21 and its inhibitory GDP/GTP exchange protein (rho GDI). *J. Cell Biol.* 120:1187–1195.

Kitano, T., M. Go, U. Kikkawa, and Y. Nishizuka. 1986. Assay and purification of protein kinase C. *Methods Enzymol.* 124:349–352.

Kosako, H., M. Amano, M. Yanagida, K. Tanabe, Y. Nishi, K. Kaibuchi, and M. Inagaki. 1997. Phosphorylation of glial fibrillary acidic protein at the same sites by cleavage furrow kinase and Rho-associated kinase. *J. Biol. Chem.* 272:10333–10336.

Kosako, H., H. Goto, M. Yanagida, K. Matsuzawa, Y. Tomono, T. Okigaki, H. Odai, K. Kaibuchi, and M. Inagaki. 1999. Specific accumulation of Rho-associated kinase at the cleavage furrow during cytokinesis; cleavage furrow-specific phosphorylation of intermediate filament. *Oncogene.* 18:2783–2788.

Kureishi, Y., S. Kobayashi, M. Amano, K. Kimura, H. Kanaide, T. Nakano, K. Kaibuchi, and M. Ito. 1997. Rho-associated kinase directly induces smooth muscle contraction through myosin light chain phosphorylation. *J. Biol. Chem.* 272:12257–12260.

Lauffenburger, D.A., and A.F. Horwitz. 1996. Cell migration: a physically integrated molecular process. *Cell.* 84:359–369.

Leung, T., E. Manser, L. Tan, and L. Lim. 1995. A novel serine/threonine kinase binding the Ras-related RhoA GTPase which translocates the kinase to peripheral membranes. *J. Biol. Chem.* 270:29051–29054.

Leung, T., X.Q. Chen, E. Manser, and L. Lim. 1996. The p160 RhoA-binding kinase ROKα is a member of a kinase family and is involved in the reorganization of the cytoskeleton. *Mol. Cell. Biol.* 16:5313–5327.

Mabuchi, I., Y. Hamaguchi, H. Fujimoto, N. Morii, M. Mishima, and S. Narumiya. 1993. A rho-like protein is involved in the organisation of the contractile ring in dividing sand dollar eggs. *Zygote.* 1:325–331.

Madaule, P., T. Furuyashiki, T. Reid, T. Ishizaki, G. Watanabe, N. Morii, and S. Narumiya. 1995. A novel partner for the GTP-bound forms of rho and rac. *FEBS Lett.* 377:243–248.

Madaule, P., M. Eda, N. Watanabe, K. Fujisawa, T. Matsuoka, H. Bito, T. Ishizaki, and S. Narumiya. 1998. Role of citron kinase as a target of the small GTPase Rho in cytokinesis. *Nature.* 394:491–494.

Matsui, T., M. Amano, T. Yamamoto, K. Chihara, M. Nakafuku, M. Ito, T. Nakano, K. Okawa, A. Iwamatsu, and K. Kaibuchi. 1996. Rho-associated kinase, a novel serine/threonine kinase, as a putative target for small GTP binding protein Rho. *EMBO (Eur. Mol. Biol. Organ.) J.* 15:2208–2216.

Matsui, T., M. Maeda, Y. Doi, S. Yonemura, M. Amano, K. Kaibuchi, S. Tsukita, and S. Tsukita. 1998. Rho-kinase phosphorylates COOH-terminal threonines of ezrin/radixin/moesin (ERM) proteins and regulates their head-to-tail association. *J. Cell Biol.* 140:647–657.

Matsumura, F., S. Ono, Y. Yamakita, G. Totsukawa, and S. Yamashiro. 1998. Specific localization of serine 19 phosphorylated myosin II during cell locomotion and mitosis of cultured cells. *J. Cell Biol.* 140:119–129.

Matsuura, Y., R.D. Possee, H.A. Overton, and D.H. Bishop. 1987. Baculovirus expression vectors: the requirements for high level expression of proteins, including glycoproteins. *J. Gen. Virol.* 68:1233–1250.

Mitchison, T.J., and L.P. Cramer. 1996. Actin-based cell motility and cell locomotion. *Cell.* 84:371–379.

Montminy, M.R., and L.M. Bilezikjian. 1987. Binding of a nuclear protein to the cyclic-AMP response element of the somatostatin gene. *Nature.* 328: 175–178.

Morii, N., and S. Narumiya. 1995. Preparation of native and recombinant *Clostridium botulinum* C3 ADP-ribosyltransferase and identification of Rho proteins by ADP-ribosylation. *Methods Enzymol.* 256:196–206.

Murata, K., K. Hirano, E. Villa-Moruzzi, D.J. Hartshorne, and D.L. Brautigan. 1997. Differential localization of myosin and myosin phosphatase subunits in smooth muscle cells and migrating fibroblasts. *Mol. Biol. Cell.* 8:663–673.

Nagafuchi, A., Y. Shirayoshi, K. Okazaki, K. Yasuda, and M. Takeichi. 1987. Transformation of cell adhesion properties by exogenously introduced E-cadherin cDNA. *Nature.* 329:341–343.

Nakai, K., Y. Suzuki, H. Kihira, H. Wada, M. Fujioka, M. Ito, T. Nakano, K. Kaibuchi, H. Shiku, and M. Nishikawa. 1997. Regulation of myosin phosphatase through phosphorylation of the myosin-binding subunit in platelet activation. *Blood.* 90:3936–3942.

Nakamura, T., T. Nishizawa, M. Hagiya, T. Seki, M. Shimonishi, A. Sugimura, K. Tashiro, and S. Shimizu. 1989. Molecular cloning and expression of human hepatocyte growth factor. *Nature.* 342:440–443.

Nishiki, T., S. Narumiya, N. Morii, M. Yamamoto, M. Fujiwara, Y. Kamata, G. Sakaguchi, and S. Kozaki. 1990. ADP-ribosylation of the rho/rac proteins induces growth inhibition, neurite outgrowth and acetylcholine esterase in cultured PC-12 cells. *Biochem. Biophys. Res. Commun.* 167:265–272.

Nishiyama, T., T. Sasaki, K. Takaishi, M. Kato, H. Yaku, K. Araki, Y. Matsuura, and Y. Takai. 1994. rac p21 is involved in insulin-induced membrane ruffling and rho p21 is involved in hepatocyte growth factor- and 12-O-tetradecanoylphorbol-13-acetate (TPA)-induced membrane ruffling in KB cells. *Mol. Cell. Biol.* 14:2447–2456.

Noda, M., C. Yasuda-Fukazawa, K. Moriishi, T. Kato, T. Okuda, K. Kurokawa, and Y. Takuwa. 1995. Involvement of rho in GTP gamma S-induced enhancement of phosphorylation of 20 kDa myosin light chain in vascular smooth muscle cells: inhibition of phosphatase activity. *FEBS Lett.* 367:246–250.

Oshiro, N., Y. Fukata, and K. Kaibuchi. 1998. Phosphorylation of moesin by Rho-associated kinase (Rho-kinase) plays a crucial role in the formation of microvilli-like structures. *J. Biol. Chem.* 273:34663–34666.

Reid, T., T. Furuyashiki, T. Ishizaki, G. Watanabe, N. Watanabe, K. Fujisawa, N. Morii, P. Madaule, and S. Narumiya. 1996. Rhotekin, a new putative target for Rho bearing homology to a serine/threonine kinase, PKN, and rhophilin in the rho-binding domain. *J. Biol. Chem.* 271:13556–13560.

Ridley, A.J., and A. Hall. 1992. The small GTP-binding protein rho regulates the assembly of focal adhesions and actin stress fibers in response to growth factors. *Cell.* 70:389–399.

Ridley, A.J., H.F. Paterson, C.L. Johnston, D. Diekmann, and A. Hall. 1992. The small GTP-binding protein rac regulates growth factor-induced membrane ruffling. *Cell.* 70:401–410.

Ridley, A.J., and A. Hall. 1994. Signal transduction pathways regulating Rho-mediated stress fiber formation: requirement for a tyrosine kinase. *EMBO (Eur. Mol. Biol. Organ.) J.* 13:2600–2610.

Sato, N., S. Yonemura, T. Obinata, S. Tsukita, and S. Tsukita. 1991. Radixin, a barbed end-capping actin-modulating protein, is concentrated at the cleavage furrow during cytokinesis. *J. Cell Biol.* 113:321–330.

Seki, T., I. Ihara, A. Sugimura, M. Shimonishi, T. Nishizawa, O. Asami, H. Hagiya, T. Nakamura, and S. Shimizu. 1990. Isolation and expression of cDNA for different forms of hepatocyte growth factor from human leukocyte. *Biochem. Biophys. Res. Commun.* 172:321–327.

Shaw, R.J., M. Henry, F. Solomon, and T. Jacks. 1998. RhoA-dependent phosphorylation and relocalization of ERM proteins into apical membrane/actin protrusions in fibroblasts. *Mol. Biol. Cell.* 9:403–419.

Shimizu, H., M. Ito, M. Miyahara, K. Ichikawa, S. Okubo, T. Konishi, M. Naka,

T. Tanaka, K. Hirano, D.J. Hartshorne, and T. Nakano. 1994. Characterization of the myosin-binding subunit of smooth muscle myosin phosphatase. *J. Biol. Chem.* 269:30407–30411.

Singer, W.D., H.A. Brown, and P.C. Sternweis. 1997. Regulation of eukaryotic phosphatidylinositol-specific phospholipase C and phospholipase D. *Annu. Rev. Biochem.* 66:475–509.

Somlyo, A. 1997. Rhomantic interludes raise blood pressure. *Nature.* 389:908–911.

Sweeney, H.L., Z. Yang, G. Zhi, J.T. Stull, and K.M. Trybus. 1994. Charge replacement near the phosphorylatable serine of the myosin regulatory light chain mimics aspects of phosphorylation. *Proc. Natl. Acad. Sci. USA.* 91:1490–1494.

Takaishi, K., A. Kikuchi, S. Kuroda, K. Kotani, T. Sasaki, and Y. Takai. 1993. Involvement of rho p21 and its inhibitory GDP/GTP exchange protein (rho GDI) in cell motility. *Mol. Cell. Biol.* 13:72–79.

Takaishi, K., T. Sasaki, M. Kato, W. Yamochi, S. Kuroda, T. Nakamura, M. Takeichi, and Y. Takai. 1994. Involvement of Rho p21 small GTP-binding protein and its regulator in the HGF-induced cell motility. *Oncogene.* 9:273–279.

Takaishi, K., T. Sasaki, T. Kameyama, S. Tsukita, S. Tsukita, and Y. Takai. 1995. Translocation of activated Rho from the cytoplasm to membrane ruffling area, cell-cell adhesion sites and cleavage furrows. *Oncogene.* 11:39–48.

Trinkle-Mulcahy, L., K. Ichikawa, D.J. Hartshorne, M.J. Siegman, and T.M. Butler. 1995. Thiophosphorylation of the 130-kDa subunit is associated with a decreased activity of myosin light chain phosphatase in alpha-toxin-permeabilized smooth muscle. *J. Biol. Chem.* 270:18191–18194.

Ueda, T., A. Kikuchi, N. Ohga, J. Yamamoto, and Y. Takai. 1990. Purification and characterization from bovine brain cytosol of a novel regulatory protein inhibiting the dissociation of GDP from and the subsequent binding of GTP to rhoB p20, a ras p21-like GTP-binding. *J. Biol. Chem.* 265:9373–9380.

Uehata, M., T. Ishizaki, H. Satoh, T. Ono, T. Kawahara, T. Morishita, H. Tamakawa, K. Yamagami, J. Inui, M. Maekawa, and S. Narumiya. 1997. Calcium sensitization of smooth muscle mediated by a Rho-associated protein kinase in hypertension. *Nature.* 389:990–994.

Van Aelst, L., and C. D'Souza-Schorey. 1997. Rho GTPases and signaling networks. *Genes Dev.* 11:2295–2322.

Watanabe, G., Y. Saito, P. Madaule, T. Ishizaki, K. Fujisawa, N. Morii, H. Mukai, Y. Ono, A. Kakizuka, and S. Narumiya. 1996. Protein kinase N (PKN) and PKN-related protein rhophilin as targets of small GTPase Rho. *Science.* 271:645–648.

Watanabe, N., P. Madaule, T. Reid, T. Ishizaki, G. Watanabe, A. Kakizuka, Y. Saito, K. Nakao, B.M. Jockusch, and S. Narumiya. 1997. p140mDia, a mammalian homolog of *Drosophila* diaphanous, is a target protein for Rho small GTPase and is a ligand for profilin. *EMBO (Eur. Mol. Biol. Organ.) J.* 16:3044–3056.

Wilson, A.K., G. Gorgas, W.D. Claypool, and P. de Lanerolle. 1991. An increase or a decrease in myosin II phosphorylation inhibits macrophage motility. *J. Cell Biol.* 114:277–283.

Yasui, Y., M. Amano, N. Inagaki, K. Nagata, H. Nakamura, H. Saya, K. Kaibuchi, and M. Inagaki. 1998. Roles of Rho-associated kinase (Rho-kinase) in cytokinesis; mutations in Rho-kinase phosphorylation sites impair cytokinetic segregation of glial filaments. *J. Cell Biol.* 143:1249–1258.